A Weighted Combining Algorithm for Spatial Multiplexing MIMO DF Relaying Systems

Kangli Zhang, *Student Member, IEEE*, Jian Wang, *Student Member, IEEE*, Jiaxin Yang, *Student Member, IEEE*, Benoit Champagne, *Senior Member, IEEE*, Fanglin Gu, and Jibo Wei, *Member, IEEE*

Abstract—**Jointly detecting the signals from the source and relay in a spatial multiplexing (SM) multiple-input multiple-output (MIMO) relaying system improves the transmit reliability significantly. However, the existing joint detection schemes for SM MIMO relaying systems, which achieve full diversity, such as the near maximum likelihood (ML) decoder, suffer from high complexity. In this paper, we propose a weighted combining (WC) algorithm, which is applied before the detector in the SM MIMO decode-and-forward relaying system. The proposed algorithm merges the received signal vectors from the source and relay into a combined signal without expanding their dimension, and formulates an equivalent MIMO channel matrix for the combined signal, resulting in a lower complexity for the subsequent detection. We analyze the performance of the proposed WC algorithm with ML detection in terms of the diversity order and computational complexity. An approximate upper bound on the symbol error probability (SEP) for the proposed algorithm is also derived. Simulation results show that in symmetric networks, the proposed WC algorithm achieves substantially lower complexity, while maintaining an SEP performance similar to that of the benchmark NML decoder. The consistency of the derived upper bound on the SEP is also verified by simulations.**

Index Terms—**Signal combining, spatial multiplexing (SM), multiple-input multiple-output (MIMO) relaying, decode-and-forward, maximum likelihood (ML) detector, pairwise error probability.**

I. INTRODUCTION

FADING is the main cause of signal distortion and outage in wireless communication networks. Relaying schemes offer an efficient way to combat signal fading (and shadowing) by providing additional transmission link capabilities. In addition, they can be used to increase network density in hotspots and extend network coverage in areas where there is little to no signal. Due to their flexible placement and cost effectiveness, relays have been widely adopted within the fourth generation (4G) LTE Advanced standard [2], [3]. Among the

available protocols for relay systems, non-regenerative amplify-and-forward (AF) and regenerative decode-and-forward (DF) are most commonly used. The former applies a linear transformation to the signals received at the relay before forwarding them to the destination, while the latter attempts to decode the receive signals and retransmit original copies.

When the nodes in the relaying systems are configured with multiple antennas, i.e., in the case of a multiple-input multiple-output (MIMO) relaying system, the transmission reliability and the spectral efficiency can be increased significantly. The MIMO relaying system integrates the advantages of MIMO and relay techniques, which further broadens its realm of application into the next generation of wireless communication systems, e.g., by enhancing the quality and uniformity of service in dense urban areas [6] or improving the transmission reliability in device-to-device (D2D) communications [7]. It has been demonstrated that by using transmit diversity techniques, such as orthogonal space-time block codes (OSTBC) [8], [9], beamforming [10]–[12] and antenna selection [13], both MIMO AF and DF relaying systems can achieve full diversity with the combining algorithms designed for single-input single-output (SISO) relaying systems [14]–[16]. However, the spectral efficiency for MIMO relaying systems using transmit diversity techniques is lower than that of spatial multiplexing (SM) MIMO relaying systems. To meet the exacting transmission requirements set forth for the fifth generation (5G) of wireless networks, the SM MIMO relaying scheme is a promising choice, since it can achieve high data rates and cooperative diversity gain simultaneously with the ML detector or its lower-complexity variants, such as the sphere decoder (SD).

In SM MIMO relaying systems, the different information signals transmitted by the source antennas are superimposed at each one of the destination antennas. As a result, the combining algorithms developed for SISO relaying systems are not efficient for SM MIMO relaying systems. One widely adopted algorithm for SM MIMO AF relaying systems is vector combining (VC), whereby the signals received from different links are concatenated prior to the detection at the destination [17], [18]. Unfortunately, the increased signal dimension in VC leads to an exponential growth in the complexity of the subsequent ML detection. To overcome this problem, a ML combining (MLC) algorithm was proposed in [19], where a combined signal vector and an equivalent channel matrix with same dimensions as those for the source-to-destination link are derived and exploited to reduce the complexity of the subsequent detection. For the case of

MIMO DF relaying systems, a near ML (NML) detector was first derived in [20] to achieve the full diversity; nevertheless, the intensive computation load of NML makes it prohibitive for practical use. Subsequently, the authors of [21] approximated the pairwise error probability (PEP) in the NML criterion with the Chernoff bound in order to transform the joint detection problem into a point-to-point MIMO detection form. Although the complexity of this modified NML (M-NML) algorithm is lower than that of NML, especially in terms of the numbers of visited nodes in the tree search process and multiply-and-accumulate operations in the real field, the complexity order for the M-NML detection is identical to that of NML, that is, $O(\Omega^{2N_s})$ where Ω and N_s denote the cardinality of the symbol constellation and the number of source antennas, respectively. Meanwhile, [19] provided an extended cooperative maximum ratio combining (EC-MRC) algorithm, which realized a significant complexity reduction to $O(\Omega^{N_s})$ at the cost of a diversity loss.

In this paper, in order to achieve a better trade-off between performance and complexity for SM MIMO DF relaying systems, we propose a weighted combining (WC) algorithm, whereby a combined signal vector and an equivalent channel matrix are derived from the received signals and corresponding channels of the different links based on a weighted linear transformation. The main virtue of the new algorithm, when compared to the above cited works, is to reduce the complexity order to $O(\Omega^{N_s})$ while preserving the same diversity as that of NML. In particular, using the estimated value of the detection error vector at the relay, the combined signal and equivalent channel matrix can be transformed into special forms which have the same dimensions as those of the received signal and channel matrix for the source-to-destination link, respectively. This dimensionality preserving approach for combining the signals from the source and the relay yields a lower complexity order of the subsequent symbol detection. Additionally, the performance gap between the proposed WC and NML algorithms can be reduced by properly selecting the value of the underlying weighting factor. We evaluate the performance of the proposed algorithm theoretically in terms of diversity order and computational complexity, and validate the findings with simulations. We also derive an approximate upper bound on the symbol error probability (SEP) based on an upper bound for the PEP. Finally, it is shown by numerical simulations that the derived upper bound provides consistency with the experimental SEP in the high SNR regime.

The rest of this paper is organized as follows. The system model is introduced in Section II, whereas the existing joint detection schemes and the proposed WC algorithm are detailed in Section III. In Section IV, the WC algorithm with ML detection is theoretically analyzed in terms of its diversity order and computational complexity, followed by the derivation of an approximate upper bound on the SEP. Simulation results are presented in Section V and conclusions are drawn in Section VI. Additional proofs are contained in Appendices.

II. SYSTEM MODEL

Consider a MIMO DF relaying system consisting of three nodes: a source (S), a relay (R) and a destination (D) as
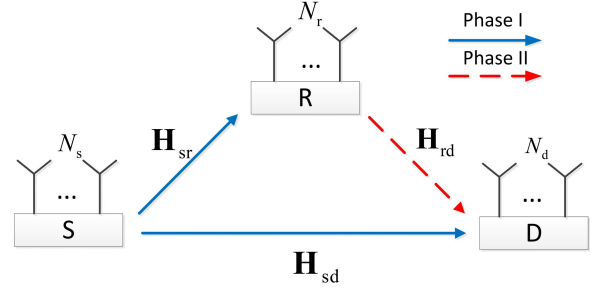

Fig. 1.   Three nodes SM MIMO DF relaying system.

depicted in Fig. 1, where nodes S, R and D are equipped with N_s, N_r and N_d antennas respectively. At R, N_{r_r} antennas are used to receive the signal from S, while N_{r_t} antennas are used for transmission to D, and $N_r = \max(N_{r_t}, N_{r_r})$. We assume that $N_s = N_{r_t}$ and the transmit antennas at S and R work in SM mode. At any given time instance, the relay-assisted transmission is completed in two time orthogonal phases. In Phase I, S broadcasts its signal to R and D, whereas in Phase II, R forwards the recovered signal to D while S keeps silent. It is further assumed that all the propagation channels are flat fading and remain approximately constant during each transmission period, and that R and D can obtain the required channel matrices of different links through the application of existing channel estimation methods [22], [23].

In Phase I, the received signals at R and D are respectively given by

$$\mathbf{y}_r = \mathbf{H}_{sr}\mathbf{x} + \mathbf{n}_r, \qquad (1)$$
$$\mathbf{y}_{d,1} = \mathbf{H}_{sd}\mathbf{x} + \mathbf{n}_{d,1}, \qquad (2)$$

where $\mathbf{x}$ denotes the $N_s \times 1$ transmitted signal vector whose entries are selected from a normalized M-ary constellation $\mathcal{X}$ of complex valued symbols with cardinality $\Omega = |\mathcal{X}|$, $\mathbf{H}_{sr}$ and $\mathbf{H}_{sd}$ represent the $N_{r_r} \times N_s$ and $N_d \times N_s$ complex-valued channel matrices for the S-R and S-D links, and $\mathbf{n}_r$ and $\mathbf{n}_{d,1}$ denote the $N_{r_r} \times 1$ and $N_d \times 1$ additive noise vectors at R and D, respectively. The entries of $\mathbf{H}_{sr}$, $\mathbf{H}_{sd}$, $\mathbf{n}_r$ and $\mathbf{n}_{d,1}$ are independent and identically distributed (i.i.d.) zero-mean circular symmetric complex Gaussian (ZMCSCG) random variables with variances σ_{sr}^2 and σ_{sd}^2 for the channel matrices and σ_r^2 and σ_d^2 for the noise vectors, respectively. At R, the source signal information contained in $\mathbf{y}_r$ is obtained by a ML decoder, yielding

$$\check{\mathbf{x}} = \arg\min_{\mathbf{x} \in \mathcal{X}^{N_s}} \|\mathbf{y}_r - \mathbf{H}_{sr}\mathbf{x}\|^2, \qquad (3)$$

where $\|\cdot\|$ denotes the 2-norm of a vector. Meanwhile, $\mathbf{y}_{d,1}$ is stored in memory at D for the subsequent combining purpose.

In Phase II, the received signal at D is given by

$$\begin{aligned} \mathbf{y}_{d,2} &= \mathbf{H}_{rd}\check{\mathbf{x}} + \mathbf{n}_{d,2} \\ &= \mathbf{H}_{rd}(\mathbf{x} + \mathbf{e}) + \mathbf{n}_{d,2}, \qquad (4) \end{aligned}$$

where $\mathbf{e} = \check{\mathbf{x}} - \mathbf{x}$ denotes the detection error vector at R, $\mathbf{H}_{rd}$ is the $N_d \times N_{r_t}$ channel matrix of the R-D link, and $\mathbf{n}_{d,2}$ is the $N_d \times 1$ additive noise vector at D in the second phase. The entries of $\mathbf{H}_{rd}$ and $\mathbf{n}_{d,2}$ are modeled as i.i.d. ZMCSCG random variables with variance σ_{rd}^2 and σ_d^2, respectively.

III. JOINT DETECTION SCHEMES FOR SM MIMO DF RELAYING SYSTEMS

In this section, we first give a brief introduction to some of the existing joint detection schemes that are available for determining the transmitted signal from S, given the noisy signal observations at D. Then, a new WC algorithm, to be used prior to the detector at D, is derived in order to achieve a better trade-off between the SEP and complexity.

A. Existing Joint Detection Schemes

To recover the original signal vector $\mathbf{x}$ transmitted by S, we need to jointly consider the noisy signals received at D during the two transmission phases, as given in (2) and (4). One way of jointly detecting the signals from S and R is to extend the cooperative maximum ratio combining scheme to MIMO relaying systems [21]. The detection metric of the resulting EC-MRC is given as

$$\tilde{\mathbf{x}}_{\text{EC-MRC}} = \arg \min_{\mathbf{x} \in \mathcal{X}^{N_s}} \left\{ \left\| \mathbf{y}_{d,1} - \mathbf{H}_{sd}\mathbf{x} \right\|^2 + \alpha \left\| \mathbf{y}_{d,2} - \mathbf{H}_{rd}\mathbf{x} \right\|^2 \right\},$$
(5)

where $0 \leq \alpha \leq 1$ controls the relative weight given to the two phases. Since the search is over $\mathcal{X}^{N_s}$, the detection complexity increases in $O(\Omega^{N_s})$. However, in EC-MRC, the detection errors at R are neglected and the effect of the S-R link is only considered through the selection of the combining factor α. Therefore, the use of EC-MRC in SM MIMO DF relaying systems does not achieve cooperative diversity.

An alternative approach to the joint signal detection problem at D is to use the NML decoder [20], with detection criterion given as

$$\tilde{\mathbf{x}}_{\text{NML}} = \arg \min_{\mathbf{x} \in \mathcal{X}^{N_s}} \left\{ \left\| \mathbf{y}_{d,1} - \mathbf{H}_{sd}\mathbf{x} \right\|^2 \right. $$
$$\left. + \min_{\check{\mathbf{x}} \in \mathcal{X}^{N_s}} \left(\left\| \mathbf{y}_{d,2} - \mathbf{H}_{rd}\check{\mathbf{x}} \right\|^2 - \sigma_d^2 \ln P(\mathbf{x} \to \check{\mathbf{x}}|\mathbf{H}_{sr}) \right) \right\}. \quad (6)$$

In this expression, $P(\mathbf{x} \to \check{\mathbf{x}}|\mathbf{H}_{sr})$ denotes the conditional PEP between $\check{\mathbf{x}}$ and $\mathbf{x}$ for the S-R link, which can be expressed as

$$P(\mathbf{x} \to \check{\mathbf{x}}|\mathbf{H}_{sr}) = Q\left(\sqrt{\frac{\|\mathbf{H}_{sr}(\check{\mathbf{x}} - \mathbf{x})\|^2}{2\sigma_r^2}} \right),$$
(7)

where

$$Q(x) = \int_x^{\infty} \exp\left[-t^2/2\right] dt, \quad x \in \mathbb{R}. \quad (8)$$

Subsequently, to avoid the difficulties posed by the evaluation of the Q-function in the solution of (6) and reformulate the detection into a point-to-point MIMO ML detection form, the authors of [21] simplified the NML detector based on the Chernoff bound approximation of (7). The detection criterion of the resulting M-NML detector is given as

$$\tilde{\mathbf{x}}_{\text{M-NML}} = \arg \min_{\mathbf{x} \in \mathcal{X}^{N_s}} \left\{ \left\| \mathbf{y}_{d,1} - \mathbf{H}_{sd}\mathbf{x} \right\|^2 \right. $$
$$\left. + \min_{\check{\mathbf{x}} \in \mathcal{X}^{N_s}} \left(\left\| \mathbf{y}_{d,2} - \mathbf{H}_{rd}\check{\mathbf{x}} \right\|^2 + \frac{\sigma_d^2}{4\sigma_r^2} \|\mathbf{H}_{sr}(\check{\mathbf{x}} - \mathbf{x})\|^2 \right) \right\}. \quad (9)$$

Equivalently, the solution to (9) can be expressed as a point-to-point MIMO ML detection problem over the extended space $\mathcal{X}^{2N_s}$, as given by [21]

$$[\tilde{\mathbf{x}}_{\text{M-NML}}^T, \tilde{\mathbf{x}}^T] = \arg \min_{\mathbf{x}_M \in \mathcal{X}^{2N_s}} \|\mathbf{y}_M - \mathbf{H}_M \mathbf{x}_M\|^2, \quad (10)$$

where

$$\mathbf{y}_M = \left[\mathbf{y}_{d,1}^T, \mathbf{y}_{d,2}^T, \mathbf{0}_{2N_r}^T \right]^T, \quad (11)$$

$$\mathbf{H}_M = \begin{bmatrix} \mathbf{H}_{sd} & \mathbf{0}_{N_d \times N_s} \\ \mathbf{0}_{N_d \times N_s} & \mathbf{H}_{rd} \\ \frac{\sigma_d}{2\sigma_r}\mathbf{H}_{sr} & -\frac{\sigma_d}{2\sigma_r}\mathbf{H}_{sr} \end{bmatrix}, \quad (12)$$

$$\mathbf{x}_M = [\mathbf{x}^T, \check{\mathbf{x}}^T]^T, \quad (13)$$

and $(\cdot)^T$ denotes transpose. In (11) and (12), $\mathbf{0}_{2N_r}$ and $\mathbf{0}_{N_d \times N_s}$ represent the $2N_r \times 1$ vector and $N_d \times N_s$ matrix with zero elements, respectively.

Although the M-NML detector in (10) avoids the computation of the Q-function, similar to the NML detector, the symbol vector to be estimated is the concatenation of $\mathbf{x}$ and $\check{\mathbf{x}}$. Consequently, the detection complexity of both schemes increases in $O(\Omega^{2N_s})$, i.e., as an exponential function of *twice* the number of transmit antennas. This increase in complexity is quite significant and limits the real-time application of these methods to small values of Ω or N_s.

B. The Proposed WC Algorithm

Considering the pros and cons of these existing joint detection schemes, we propose a WC algorithm to be applied before the ML detection at D, which offers a better trade-off between the complexity and diversity performance. We first extend the joint detector in (9) to a weighted NML detector (W-NML). Specifically, upon substituting $\check{\mathbf{x}}$ by $\mathbf{x} + \mathbf{e}$ and replacing the factor $\frac{\sigma_d^2}{4\sigma_r^2}$ in (9) with a positive weighting factor w, we obtain

$$\tilde{\mathbf{x}}_{\text{W-NML}} = \arg \min_{\mathbf{x} \in \mathcal{X}^{N_s}} \left\{ \left\| \mathbf{y}_{d,1} - \mathbf{H}_{sd}\mathbf{x} \right\|^2 \right. $$
$$\left. + \min_{\mathbf{e} \in \mathcal{E}^{N_s}} \left(\left\| \mathbf{y}_{d,2} - \mathbf{H}_{rd}(\mathbf{x} + \mathbf{e}) \right\|^2 + w \|\mathbf{H}_{sr}\mathbf{e}\|^2 \right) \right\}, \quad (14)$$

where $\mathcal{E} = \{e = x - y | x, y \in \mathcal{X}\}$ denotes the set of possible values for the individual symbol errors, and the purpose of w will be further discussed below. This extension enables the detector to take more flexible forms while the system performance can be improved by properly selecting w, as will be explained. Secondly, the discrete set of values for the error vector $\mathbf{e}$, i.e., $\mathcal{E}^{N_s}$ is relaxed to the complex space $\mathbb{C}^{N_s}$, so that the detector in (14) can be approximated as

$$\tilde{\mathbf{x}}_{\text{WC}} = \arg \min_{\mathbf{x} \in \mathcal{X}^{N_s}} \left\{ \left\| \mathbf{y}_{d,1} - \mathbf{H}_{sd}\mathbf{x} \right\|^2 \right. $$
$$\left. + \min_{\mathbf{e} \in \mathbb{C}^{N_s}} \left(\left\| \mathbf{y}_{d,2} - \mathbf{H}_{rd}(\mathbf{x} + \mathbf{e}) \right\|^2 + w \|\mathbf{H}_{sr}\mathbf{e}\|^2 \right) \right\}. \quad (15)$$

The above formulation allows us to evaluate the inner minimization in closed form. Indeed, we can find an optimal value of $\mathbf{e}$ by equating the Wirtinger derivative of the inner term with respect to (w.r.t.) $\mathbf{e}^*$ to zero [24], i.e.,

$$\frac{\partial}{\partial \mathbf{e}^*} \left(\left\| \mathbf{y}_{d,2} - \mathbf{H}_{rd}(\mathbf{x} + \mathbf{e}) \right\|^2 + w \|\mathbf{H}_{sr}\mathbf{e}\|^2 \right) = \mathbf{0}. \quad (16)$$

This yields

$$\mathbf{e}_{\min} = \Xi \mathbf{H}_{rd}^H \left(\mathbf{y}_{d,2} - \mathbf{H}_{rd}\mathbf{x} \right), \qquad (17)$$

where we define matrix

$$\Xi = \left(\mathbf{H}_{rd}^H \mathbf{H}_{rd} + w \mathbf{H}_{sr}^H \mathbf{H}_{sr} \right)^{-1}, \qquad (18)$$

while $(\cdot)^*$ and $(\cdot)^H$ denote the conjugate and conjugate transpose operations, respectively. Note that condition $N_s = N_{r_t}$ is assumed in Section II to guarantee the existence of Ξ. Substituting (17) back into (15), the latter can be equivalently expressed as a point-to-point MIMO ML detection form, as given by

$$
\begin{aligned}
\tilde{\mathbf{x}}_{WC} = & \arg \min_{\mathbf{x} \in \mathcal{X}^{N_s}} \left\{ \left\| \mathbf{y}_{d,1} - \mathbf{H}_{sd}\mathbf{x} \right\|^2 \right. \\
& + \left\| \mathbf{y}_{d,2} - \mathbf{H}_{rd}\mathbf{x} - \mathbf{H}_{rd}\Xi\mathbf{H}_{rd}^H \left(\mathbf{y}_{d,2} - \mathbf{H}_{rd}\mathbf{x} \right) \right\|^2 \\
& \left. + w \left\| \mathbf{H}_{sr}\Xi\mathbf{H}_{rd}^H \left(\mathbf{y}_{d,2} - \mathbf{H}_{rd}\mathbf{x} \right) \right\|^2 \right\} \\
= & \arg \min_{\mathbf{x} \in \mathcal{X}^{N_s}} \left\{ \mathbf{y}_{d,1}^H \mathbf{y}_{d,1} + \mathbf{y}_{d,2}^H \mathbf{y}_{d,2} - \mathbf{y}_{d,2}^H \mathbf{H}_{rd}\Xi\mathbf{H}_{rd}^H \mathbf{y}_{d,2} \right. \\
& - \mathbf{x}^H \left(\mathbf{H}_{sd}^H \mathbf{y}_{d,1} + w \mathbf{H}_{sr}^H \mathbf{H}_{sr}\Xi\mathbf{H}_{rd}^H \mathbf{y}_{d,2} \right) \\
& - \left(\mathbf{y}_{d,1}^H \mathbf{H}_{sd} + w \mathbf{y}_{d,2}^H \mathbf{H}_{rd}\Xi\mathbf{H}_{sr}^H \mathbf{H}_{sr} \right) \mathbf{x} \\
& \left. + \mathbf{x}^H \left(\mathbf{H}_{sd}^H \mathbf{H}_{sd} + w \mathbf{H}_{sr}^H \mathbf{H}_{sr}\Xi\mathbf{H}_{rd}^H \mathbf{H}_{rd} \right) \mathbf{x} \right\} \\
= & \arg \min_{\mathbf{x} \in \mathcal{X}^{N_s}} \left\{ \mathbf{y}_C^H \mathbf{y}_C - \mathbf{x}^H \mathbf{H}_E^H \mathbf{y}_C - \mathbf{y}_C^H \mathbf{H}_E \mathbf{x} + \mathbf{x}^H \mathbf{H}_E^H \mathbf{H}_E \mathbf{x} \right\} \\
= & \arg \min_{\mathbf{x} \in \mathcal{X}^{N_s}} \left\| \mathbf{y}_C - \mathbf{H}_E\mathbf{x} \right\|^2, \qquad (19)
\end{aligned}
$$

where the equivalent channel matrix $\mathbf{H}_E \in \mathbb{C}^{N_s \times N_s}$ and combined signal vector $\mathbf{y}_C \in \mathbb{C}^{N_d}$ satisfy

$$\mathbf{H}_E^H \mathbf{H}_E = \mathbf{H}_{sd}^H \mathbf{H}_{sd} + w \mathbf{H}_{sr}^H \mathbf{H}_{sr}\Xi\mathbf{H}_{rd}^H \mathbf{H}_{rd}, \qquad (20)$$

$$\mathbf{H}_E^H \mathbf{y}_C = \mathbf{H}_{sd}^H \mathbf{y}_{d,1} + w \mathbf{H}_{sr}^H \mathbf{H}_{sr}\Xi\mathbf{H}_{rd}^H \mathbf{y}_{d,2}, \qquad (21)$$

respectively. In practice, these quantities can be efficiently calculated as follows,

$$\mathbf{H}_E = \text{Chol} \left(\mathbf{H}_{sd}^H \mathbf{H}_{sd} + w \mathbf{H}_{sr}^H \mathbf{H}_{sr}\Xi\mathbf{H}_{rd}^H \mathbf{H}_{rd} \right), \qquad (22)$$

$$\mathbf{y}_C = \left(\mathbf{H}_E^H \right)^{-1} \left(\mathbf{H}_{sd}^H \mathbf{y}_{d,1} + w \mathbf{H}_{sr}^H \mathbf{H}_{sr}\Xi\mathbf{H}_{rd}^H \mathbf{y}_{d,2} \right), \quad (23)$$

where $\text{Chol}(\mathbf{X})$ denotes the right Cholesky factor of $\mathbf{X}$. In this way, we obtain an upper triangular form for $\mathbf{H}_E$, which is particularly suitable for the reduced-complexity detection, such as SD.

We next discuss the selection of the weighting factor w, which is introduced in (14) to modify the weight given to the detection errors at R in the detection metric. Since relays are commonly utilized when the quality of the S-R-D link is comparable or better than that of the S-D link, only the case that $\min(\text{SNR}_{sr}, \text{SNR}_{rd}) \geqslant \text{SNR}_{sd}$ is considered here. In effect, w can be used to adjust the proportions in which the direct S-D and cooperative S-R-D links contribute to the detection metric. For instance, when the SNR of the S-R-D link is better than that of the S-D link, the weight given to the former should be increased in computing the equivalent channel matrix (22) and combined signal vector (23), and vice

versa. Since w is a multiplicative factor for terms related to the S-R-D link in (15), (22) and (23), it should be monotonically increasing with the SNR of the S-R link and decreasing with that of the S-D link. Based on the above considerations and abundant simulation results, we propose the selection criterion for w as

$$
w^* = \begin{cases}
\frac{1}{2} \left\lfloor \frac{\sigma_{sr}^2/\sigma_r^2}{\sigma_{sd}^2/\sigma_d^2} \right\rfloor \approx \frac{1}{2} \left\lfloor \frac{N_d\sigma_d^2 \text{Tr}(\mathbf{H}_{sr}^H \mathbf{H}_{sr})}{N_{r_r}\sigma_r^2 \text{Tr}(\mathbf{H}_{sd}^H \mathbf{H}_{sd})} \right\rfloor \\
\quad when \ \max(\text{SNR}_{sr}, \text{SNR}_{rd}) > \text{SNR}_{sd}, \\
1.5 \ when \ \text{SNR}_{sr} = \text{SNR}_{rd} = \text{SNR}_{sd},
\end{cases} \qquad (24)
$$

where $\lfloor x \rfloor$ represents greatest integer which is less than or equal to x, $\text{Tr}(\cdot)$ denotes the trace of a matrix. Note that the quantities $\text{Tr}(\mathbf{H}_{sr}^H \mathbf{H}_{sr})/(N_{r_r}N_s)$ and $\text{Tr}(\mathbf{H}_{sd}^H \mathbf{H}_{sd})/(N_s N_d)$ are used to estimate σ_{sr}^2 and σ_{sd}^2 at D, respectively. Although this selection for w cannot be theoretically proved optimal, the selected value of w makes it possible to adjust the detection metric as the channel conditions change over time. The effectiveness of this approach has been demonstrated through exhaustive series of computer simulations for various application scenarios, where the choice of w in (24) provides superior SEP performance most of the time, as will be further discussed in Section V-A.

The proposed WC algorithm is summarized in Algorithm 1. Finally, with the computed values $\mathbf{y}_C$ and $\mathbf{H}_E$, the MIMO detection in (19) can be implemented by the ML detector or the SD [25].

Algorithm 1 WC Algorithm

1: Compute w according to (24);
2: Compute the matrix products $\mathbf{H}_{sd}^H \mathbf{H}_{sd}$, $\mathbf{H}_{sr}^H \mathbf{H}_{sr}$ and $\mathbf{H}_{rd}^H \mathbf{H}_{rd}$;
3: Use the results from Step 1 and 2 to compute Ξ based on (18);
4: Compute the equivalent channel matrix $\mathbf{H}_E$ in (22) by Cholesky decomposition;
5: Compute the combined signal $\mathbf{y}_C$ in (23) using $\mathbf{H}_E$ from Step 4 and the received signals $\mathbf{y}_{d,1}$ and $\mathbf{y}_{d,2}$ in the two transmission phases.

IV. PERFORMANCE AND COMPLEXITY ANALYSIS

In this section, we first derive an approximate upper bound on the PEP for the proposed WC algorithm with ML detection. Thereafter, the diversity order and an approximate upper bound on the SEP for SM MIMO DF relaying systems employing the WC algorithm and ML detector are presented. Finally, we analyze the computational complexity of different joint detection schemes, including selected schemes from the literature and the proposed WC algorithm with ML detection.

A. Approximate Upper Bound on PEP

Let $\hat{\mathbf{x}}$ denote the erroneously detected signal vector at D. According to the definition in [26], the PEP for ML detection with the WC algorithm can be calculated by

$$P(\mathbf{x} \to \hat{\mathbf{x}}) = P \left(m \left(\hat{\mathbf{x}} \right) < m \left(\mathbf{x} \right) \right), \qquad (25)$$

$$P(\mathbf{x} \to \hat{\mathbf{x}}) < \begin{cases} \frac{1}{2}\left(1 + \frac{\|\mathbf{t}\|^2\sigma_{\text{sd}}^2}{4\sigma_{\text{d}}^2}\right)^{-N_{\text{d}}} \prod_{\lambda_i=1}^{N_{\text{s}}} \int \left(1 + \frac{(1+\lambda_i)\lambda_i\|\mathbf{t}\|^2\sigma_{\text{sr}}^2 w}{4\sigma_{\text{r}}^2}\right)^{-1} f(\lambda_i)d\lambda_i, & N_{\text{d}} \geqslant N_{\text{r}_{\text{r}}} = N_{\text{s}} \\ \frac{1}{2}\left(1 + \frac{\|\mathbf{t}\|^2\sigma_{\text{sd}}^2}{4\sigma_{\text{d}}^2}\right)^{-N_{\text{d}}} \prod_{\eta_i=1}^{N_{\text{s}}} \int \left(1 + \frac{(2-\eta_i)\eta_i\|\mathbf{t}\|^2\sigma_{\text{rd}}^2}{4\sigma_{\text{r}}^2}\right)^{-1} f(\eta_i)d\eta_i, & N_{\text{r}_{\text{r}}} \geqslant N_{\text{d}} = N_{\text{s}} \end{cases} \tag{36}$$

where we define

$$m(\mathbf{x}) = \left\|\mathbf{y}_{\text{d},1} - \mathbf{H}_{\text{sd}}\mathbf{x}\right\|^2$$
$$+ \left\|\mathbf{y}_{\text{d},2} - \mathbf{H}_{\text{rd}}\mathbf{x} - \mathbf{H}_{\text{rd}}\Xi\mathbf{H}_{\text{rd}}^H\left(\mathbf{y}_{\text{d},2} - \mathbf{H}_{\text{rd}}\mathbf{x}\right)\right\|^2$$
$$+ w\left\|\mathbf{H}_{\text{sr}}\Xi\mathbf{H}_{\text{rd}}^H\left(\mathbf{y}_{\text{d},2} - \mathbf{H}_{\text{rd}}\mathbf{x}\right)\right\|^2 \tag{26}$$

as the detection metric, which is equal to $\|\mathbf{y}_{\text{C}} - \mathbf{H}_{\text{E}}\mathbf{x}\|^2$ according to (19). Substituting (2) and (4) into (26) along with some manipulations, the conditional PEP given the various channel matrices and the detection error vector at R can be expressed as

$$P(\mathbf{x} \to \hat{\mathbf{x}}|\mathbf{H}_{\text{sd}}, \mathbf{H}_{\text{sr}}, \mathbf{H}_{\text{rd}}, \mathbf{e})$$
$$= P\left(\Re\left[\mathbf{t}^H\left(\mathbf{H}_{\text{sd}}^H\mathbf{n}_{\text{d},1} + w\mathbf{H}_{\text{sr}}^H\mathbf{H}_{\text{sr}}\Xi\mathbf{H}_{\text{rd}}^H\mathbf{n}_{\text{d},2}\right)\right] < -a-b\right), \tag{27}$$

where

$$\mathbf{t} = \mathbf{x} - \hat{\mathbf{x}}, \tag{28}$$
$$a = \frac{1}{2}\mathbf{t}^H\left(\mathbf{H}_{\text{sd}}^H\mathbf{H}_{\text{sd}} + w\mathbf{H}_{\text{rd}}^H\mathbf{H}_{\text{rd}}\Xi\mathbf{H}_{\text{sr}}^H\mathbf{H}_{\text{sr}}\right)\mathbf{t} \geq 0, \tag{29}$$
$$b = \Re\left[w\mathbf{t}^H\mathbf{H}_{\text{rd}}^H\mathbf{H}_{\text{rd}}\Xi\mathbf{H}_{\text{sr}}^H\mathbf{H}_{\text{sr}}\mathbf{e}\right], \tag{30}$$

and $\Re[\cdot]$ stands for the real part of its argument. Since $\Re\left[\mathbf{t}^H\left(\mathbf{H}_{\text{sd}}^H\mathbf{n}_{\text{d},1} + w\mathbf{H}_{\text{sr}}^H\mathbf{H}_{\text{sr}}\Xi\mathbf{H}_{\text{rd}}^H\mathbf{n}_{\text{d},2}\right)\right]$ in (27) is a Gaussian random variable with zero mean and variance $\tilde{\sigma}^2$, as given by

$$\tilde{\sigma}^2 = \frac{\sigma_{\text{d}}^2}{2}\mathbf{t}^H\left(\mathbf{H}_{\text{sd}}^H\mathbf{H}_{\text{sd}} + w^2\mathbf{H}_{\text{sr}}^H\mathbf{H}_{\text{sr}}\Xi\mathbf{H}_{\text{rd}}^H\mathbf{H}_{\text{rd}}\Xi\mathbf{H}_{\text{sr}}^H\mathbf{H}_{\text{sr}}\right)\mathbf{t}, \tag{31}$$

(27) can be further written as

$$P(\mathbf{x} \to \hat{\mathbf{x}}|\mathbf{H}_{\text{sd}}, \mathbf{H}_{\text{sr}}, \mathbf{H}_{\text{rd}}, \mathbf{e}) = Q\left(\frac{a+b}{\tilde{\sigma}}\right). \tag{32}$$

From (29)-(32) we observe that it is difficult to compute the PEP for ML detection with the WC algorithm by directly averaging (32) w.r.t. $\mathbf{H}_{\text{sd}}$, $\mathbf{H}_{\text{sr}}$, $\mathbf{H}_{\text{rd}}$ and $\mathbf{e}$. The PEP is thereby approximately calculated in stages through the use of upper bounds. First, eliminating the random effect of $\mathbf{e}$ in (32), we have the following proposition.

Proposition 1: The conditional PEP based on $\mathbf{H}_{\text{sd}}$, $\mathbf{H}_{\text{sr}}$ and $\mathbf{H}_{\text{rd}}$ for ML detection with the WC algorithm can be upper bounded as follows in the high SNR regime for the S-R or S-D links:

$$P(\mathbf{x} \to \hat{\mathbf{x}}|\mathbf{H}_{\text{sd}}, \mathbf{H}_{\text{sr}}, \mathbf{H}_{\text{rd}})$$
$$< \frac{1}{2}\exp\left[-\frac{1}{4\sigma_{\text{d}}^2}\mathbf{t}^H(\mathbf{H}_{\text{sd}}^H\mathbf{H}_{\text{sd}}\right.$$
$$\left. + w(\mathbf{I}_{N_{\text{r}_{\text{t}}}} + \mathbf{H}_{\text{rd}}^H\mathbf{H}_{\text{rd}}\Xi)\mathbf{H}_{\text{rd}}^H\mathbf{H}_{\text{rd}}\Xi\mathbf{H}_{\text{sr}}^H\mathbf{H}_{\text{sr}})\mathbf{t}\right], \tag{33}$$

where $\mathbf{I}_N$ denotes the $N \times N$ identity matrix.

Proof : see Appendix A.

In (33), $\mathbf{H}_{\text{rd}}^H\mathbf{H}_{\text{rd}}\Xi$ is a square matrix, which has the following Schur decomposition form

$$\mathbf{H}_{\text{rd}}^H\mathbf{H}_{\text{rd}}\Xi = \mathbf{U}\mathbf{T}\mathbf{U}^H, \tag{34}$$

where $\mathbf{U}$ and $\mathbf{T}$ respectively denote a unitary matrix and an upper-triangular matrix whose diagonal elements are the eigenvalues of $\mathbf{H}_{\text{rd}}^H\mathbf{H}_{\text{rd}}\Xi$, i.e., $\lambda_i \in [0, 1]$, $i = 1, \ldots, N_{\text{s}}$ when $N_{\text{d}}, N_{\text{r}_{\text{r}}} \geqslant N_{\text{s}}$. Substituting (34) into the right side of (33), the approximate upper bound on the conditional PEP can be rewritten as

$$P(\mathbf{x} \to \hat{\mathbf{x}}|\mathbf{H}_{\text{sd}}, \mathbf{H}_{\text{sr}}, \mathbf{H}_{\text{rd}})$$
$$< \frac{1}{2}\exp\left[-\frac{1}{4\sigma_{\text{d}}^2}\mathbf{t}^H(\mathbf{H}_{\text{sd}}^H\mathbf{H}_{\text{sd}}\right.$$
$$\left. + w\mathbf{U}(\mathbf{I}_{N_{\text{r}_{\text{t}}}} + \mathbf{T})\mathbf{T}\mathbf{U}^H\mathbf{H}_{\text{sr}}^H\mathbf{H}_{\text{sr}})\mathbf{t}\right]. \tag{35}$$

Finally, by averaging (35) over $\mathbf{H}_{\text{sd}}$, $\mathbf{H}_{\text{sr}}$, $\mathbf{U}$ and $\mathbf{T}$, we arrive at the following proposition.

Proposition 2: The upper bound on the PEP for ML detection with the WC algorithm in the high SNR regime for the S-R or S-D links can be expressed as in (36) at the top of this page, where $\eta_i \in [0, 1]$, $i = 1, \ldots, N_{\text{s}}$ and $f(\cdot)$ denote the eigenvalue of the square matrix $w\mathbf{H}_{\text{sr}}^H\mathbf{H}_{\text{sr}}\Xi$ and the probability density function (PDF) of the corresponding argument, respectively.

Proof : see Appendix B.

Based on (18), matrices $\mathbf{H}_{\text{rd}}^H\mathbf{H}_{\text{rd}}\Xi$ and $w\mathbf{H}_{\text{sr}}^H\mathbf{H}_{\text{sr}}\Xi$ are Jacobi-MANOVA ensembles, the joint PDF of whose eigenvalues can be derived as follows according to [30]:

$$g(x_1, \ldots, x_{N_{\text{s}}})$$
$$= C\Delta^2(x)\prod_{i=1}^{N_{\text{s}}}x_i^{\alpha}(1 - x_i)^{\beta}(1 + (\sigma^{-1} - 1)x_i)^{-(\alpha+\beta+2N_{\text{s}})}, \tag{37}$$

where $C = 1/\det_{N_{\text{s}}}[\int_0^1 t^{j+k+\alpha-2}(1-t)^{\beta}(1+(\sigma^{-1} - 1)t)^{-(\alpha+\beta+2N_{\text{s}})}dt]$, $\Delta(x) = \prod_{1\leqslant i<j\leqslant N_s} x_i - x_j$ is the Vandermonde determinant of vector $[x_1, x_2, \ldots, x_{N_s}]$, $\alpha = N_{\text{d}} - N_{\text{s}}$, $\beta = N_{\text{r}_{\text{r}}} - N_{\text{s}}$, $\sigma = \sigma_{\text{rd}}^2/(w\sigma_{\text{sr}}^2)$ when $x_i = \lambda_i$ and $\alpha = N_{\text{r}_{\text{r}}} - N_{\text{s}}$, $\beta = N_{\text{d}} - N_{\text{s}}$, $\sigma = w\sigma_{\text{sr}}^2/\sigma_{\text{rd}}^2$ when $x_i = \eta_i$. Here $\det_N[a(j, k)]$ represents the determinant of a $N \times N$ matrix $\mathbf{A}[a(j, k)]$ with the (j, k)th element given by $a(j, k)$. Therefore the marginal PDF $f(\lambda_i)$ and $f(\eta_i)$ in (36) can be calculated by integrating (37) over the remaining eigenvalues,

for simplicity we only provide $f(x_i)$ for $N_s = 2$ as

$$f(x_i) = C \sum_{l=1}^{N_s} \det_{N_s} \left[\phi_{j,k}^{l,i}(x) \right], \quad i = 1, 2 \tag{38}$$

where $\phi_{j,k}^{l,i}(x)$ is given in (39) at the bottom of this page.

B. Diversity Analysis and Approximate Upper Bound on SEP

It can be observed from (36) that the approximate upper bound on the PEP is the product of two terms, one associated with the S-D link with diversity order N_d [26], and the other associated with the S-R-D link which is the product of PEP for the eigenvalues λ_i or η_i. Since each λ_i or η_i can provide one diversity order, the diversity order for the S-R-D link is equal to the number of eigenvalues, i.e., N_s when $\min(N_d, N_{r_r}) = N_s$. As the data transmissions over these links are independent, the diversity order of the SM MIMO DF relaying system with the WC algorithm is the sum of that for each link, i.e., $N_d + N_s$ when $\min(N_{r_r}, N_d) = N_s$.

It is difficult to derive the exact SEP[1] for the MIMO relaying systems with the ML detection. However, its upper bound can be obtained from the PEP according to [26] as follows:

$$P_s \leqslant \frac{1}{N_s} \sum_{\mathbf{x}} P_T(\mathbf{x}) \sum_{\mathbf{x} \neq \hat{\mathbf{x}}} n_e(\mathbf{x} \to \hat{\mathbf{x}}) P(\mathbf{x} \to \hat{\mathbf{x}}), \tag{40}$$

where P_s denotes the average SEP, $P_T(\mathbf{x})$ represents the probability that the signal vector $\mathbf{x}$ is transmitted, $n_e(\mathbf{x} \to \hat{\mathbf{x}})$ is the number of symbol errors when $\mathbf{x}$ is erroneously detected as another signal vector $\hat{\mathbf{x}}$, and $P(\mathbf{x} \to \hat{\mathbf{x}})$ is the PEP. For simplicity, let us assume that $P_T(\mathbf{x})$ follows an equiprobable distribution and consider the most likely circumstance that $n_e(\mathbf{x} \to \hat{\mathbf{x}}) = 1$ and $\|\mathbf{t}\|_{\min} = \min_{x_1, x_2 \in X} |x_1 - x_2|$. Under these conditions, the approximate upper bound on the SEP can be calculated by replacing the PEP in (40) with the approximate upper bound on the PEP given in (36), which yields the upper bound on SEP given in (41) at the bottom of this page, where c stands for the number of symbols which have the minimum distance to a pre-selected symbol in the constellation X. Table I lists the values of c for different transmit constellations of interest. In particular, the value of c corresponding to 16QAM

[1] A single symbol error occurs when a particular entry in $\hat{\mathbf{x}}$ is different from the corresponding entry in $\mathbf{x}$.

TABLE I
VALUES OF PARAMETER c FOR DIFFERENT TRANSMIT CONSTELLATIONS

Transmit Constellation	BPSK	QPSK	8PSK	16QAM
c	1	2	2	3

is computed by averaging symbols with different amplitudes in the constellation.

C. Computational Complexity Analysis

Next, we analyze the computational complexity of existing detection schemes from the literature as well as that of the proposed WC algorithm in terms of the number of complex multiplications (CM). In order to achieve a fair comparison, the ML detector is used in connection with our proposed WC algorithm. The complexity evaluation is carried out according to the following guidelines:

- The Cholesky decomposition of an $N \times N$ symmetric positive-definite complex-valued matrix requires $3.5N^3$ CM [27];
- The inverse of an $N \times N$ complex-valued matrix requires $4N^3$ CM [27];
- The ML detection for a MIMO system with M transmit and N receive antennas requires $N(M + 1)\Omega^M$ CM [28].

Note that the Cholesky decomposition also provides an approach for extracting the square root of a matrix. Thus for the EC-MRC scheme [21], the calculation of the equivalent channel matrix and combined signal vector requires $7.5N_s^3 + N_s^2 N_d + N_r^2 N_d + N_s N_d + N_r N_d + N_s^2$ CM, while the ML detection requires $N_s(N_s + 1)\Omega^{N_s}$ CM. Similarly, the proposed WC algorithm requires $7.5N_s^3 + 6N_r^3 + N_s^2 N_r + N_r^2 N_d + N_s^2 N_d + N_s N_d + N_r N_d + N_r^2 + N_s^2$ CM to obtain the equivalent channel matrix and combined signal vector, among which $5N_r^3 + N_s^2 N_r + N_r^2 N_d$ CM are spent on computing $w \mathbf{H}_{sr}^H \mathbf{H}_{sr} \Xi$, while the detection complexity is $N_s(N_s + 1)\Omega^{N_s}$. In contrast, the ML detection for M-NML requires $(2N_s + 1)(2N_d + N_r)\Omega^{2N_s}$ CM. NML requires $(N_r N_s + N_r)\Omega^{2N_s}$ CM to first compute the PEP at R, and then $\left[N_d(N_s + 1)\Omega^{N_s} \right]^2$ CM to perform the ML detection. The total computational complexities of all the above schemes are summarized in Table II.

We can observe from Table II that the complexities of the proposed WC algorithm and EC-MRC are mostly determined by the ML detection, which is an exponential function of

$$\phi_{j,k}^{l,i}(x) = \begin{cases} x^{\alpha+j+k-2}(1-x)^{\beta}(1+(\sigma^{-1}-1)x)^{-(\alpha+\beta+2N_s)}, & j = l \\ \int_x^1 t^{j+k+\alpha-2}(1-t)^{\beta}(1+(\sigma^{-1}-1)t)^{-(\alpha+\beta+2N_s)}dt, & j \neq l, \quad i = 1 \\ \int_0^x t^{j+k+\alpha-2}(1-t)^{\beta}(1+(\sigma^{-1}-1)t)^{-(\alpha+\beta+2N_s)}dt, & j \neq l, \quad i = 2 \end{cases} \tag{39}$$

$$P_s < \begin{cases} \dfrac{c}{2}\left(1 + \dfrac{\|\mathbf{t}\|_{\min}^2 \sigma_{sd}^2}{4\sigma_d^2}\right)^{-N_d} \prod_{\lambda_i=1}^{N_s} \int \left(1 + \dfrac{(1+\lambda_i)\lambda_i \|\mathbf{t}\|_{\min}^2 \sigma_{sr}^2 w}{4\sigma_r^2}\right)^{-1} f(\lambda_i) d\lambda_i, & N_d \geqslant N_{r_r} = N_s \\ \dfrac{c}{2}\left(1 + \dfrac{\|\mathbf{t}\|_{\min}^2 \sigma_{sd}^2}{4\sigma_d^2}\right)^{-N_d} \prod_{\eta_i=1}^{N_s} \int \left(1 + \dfrac{(2-\eta_i)\eta_i \|\mathbf{t}\|_{\min}^2 \sigma_{rd}^2}{4\sigma_r^2}\right)^{-1} f(\eta_i) d\eta_i, & N_{r_r} \geqslant N_d = N_s \end{cases} \tag{41}$$

TABLE II
COMPUTATIONAL COMPLEXITIES OF DIFFERENT JOINT DETECTION SCHEMES

Joint Detection Scheme	Computational Complexity (in CM)
EC-MRC	$(N_s^2 + N_s)\Omega^{N_s} + 7.5N_s^3 + N_s^2 N_d + N_r^2 N_d + N_s N_d + N_r N_d + N_s^2$
WC with ML detection	$(N_s^2 + N_s)\Omega^{N_s} + 7.5N_s^3 + 6N_r^3 + N_s^2 N_r + N_r^2 N_d + N_s^2 N_d + N_s N_d + N_r N_d + N_r^2 + N_s^2$
M-NML	$(4N_s N_d + 2N_s + 2N_s N_r + N_r)\,\Omega^{2N_s}$
NML	$\left(N_r N_s + N_r + N_d^2(N_s + 1)^2\right)\Omega^{2N_s}$

TABLE III
SEP OF WC ALGORITHM USING DIFFERENT VALUES OF w FOR COMMONLY ADOPTED
NETWORK TOPOLOGIES WITH 16QAM CONSTELLATION, $N = 2$

Network Topology	w	$\text{SNR}_{sd} = 8\text{dB}$	$\text{SNR}_{sd} = 16\text{dB}$	$\text{SNR}_{sd} = 24\text{dB}$
$d_{sd} = \sqrt{2}d_{sr} = \sqrt{2}d_{rd}$	0.25	0.1253	$1.76e^{-3}$	$3.9e^{-6}$
	1	0.1049	$8.71e^{-4}$	$1.2e^{-6}$
	2	0.0992	$7.66e^{-4}$	$6e^{-7}$
	1.5	0.0948	$7.31e^{-4}$	$5e^{-7}$
$d_{sd} = 2d_{sr} = d_{rd}$	0.25	0.1496	$1.93e^{-3}$	$1.8e^{-6}$
	1	0.1379	$1.24e^{-3}$	$1.8e^{-6}$
	2	0.1106	$1.26e^{-3}$	$2.3e^{-6}$
	5.5	0.1104	$1.16e^{-3}$	$9e^{-7}$
$d_{sd} = d_{sr} = 2d_{rd}$	0.25	0.1898	$3.29e^{-3}$	$6.2e^{-6}$
	1	0.1053	$2.97e^{-3}$	$4.9e^{-6}$
	2	0.1787	$5.09e^{-3}$	$8.4e^{-6}$
	0.5	0.1399	$2.36e^{-3}$	$2.1e^{-6}$

the number of transmit antennas N_s, scaled by a multiplier which is only a function of the number of transmit antennas at S. Whereas for the NML and M-NML, the complexities are exponential functions of *twice* the number of transmit antennas, scaled by multipliers which depend on the numbers of antennas at different nodes. Consequently, NML and M-NML have significantly higher complexities than EC-MRC and the proposed WC algorithm. Numerical evaluation of the computational complexity for these schemes is further discussed in the next section.

V. SIMULATION RESULTS AND DISCUSSIONS

In this section, the performance of the proposed WC algorithm with ML detection is evaluated by simulation and the analytical results derived in Section IV are validated. We consider a SM MIMO DF relaying system, as illustrated in Fig. 1, with identical number of antennas at each node, i.e., $N_s = N_r = N_d \equiv N$. The radio channels between the various pairs of antennas in the S-R, R-D and S-D links are modeled as flat-fading MIMO Rayleigh channels. We first evaluate the SEP performance of the WC algorithm with ML detection and investigate the effects of network topology and modulation order on the accuracy of the derived upper bound (41) in the high SNR regime and the effect of the antenna number on the diversity order, respectively. Then the computational complexities of the WC algorithm with ML detection and the joint detection schemes introduced in Section III-A are compared, using both the results of CM analysis (Table II) and average simulation times. In the SEP simulation, the results are averaged over 10^9 Monte Carlo experiments. For each experiment, the randomly selected channels remain static over the duration of the data transmission, which lasts for 100 symbols. The variances of the additive noise at R and D in (1), (2) and (4) are normalized to one, i.e., $\sigma_r^2 = \sigma_d^2 = 1$. The

average SNR for each link is therefore equal to the variance of the corresponding channel matrix entries, i.e., $\text{SNR}_{sd} = \sigma_{sd}^2$, $\text{SNR}_{sr} = \sigma_{sr}^2$ and $\text{SNR}_{rd} = \sigma_{rd}^2$. Considering the path loss model, we set $\sigma_{sd}^2 = Pd_{sd}^{-u}$, $\sigma_{sr}^2 = Pd_{sr}^{-u}$ and $\sigma_{rd}^2 = Pd_{rd}^{-u}$ [29], where d_{sd}, d_{sr} and d_{rd} are the transmit distances for the S-D, S-R and R-D links, respectively, and P and u respectively denote the transmit power at S and R and the path loss exponent, which is selected as $u = 3.5$ to model the urban and suburban areas. A symmetric network configuration $d_{sd} = d_{sr} = d_{rd}$ is considered throughout, except for Table III and Fig. 5.

A. SEP Performance and Approximate Upper Bound

Tables III and IV provide the SEP of the proposed WC algorithm with ML detection with different values of the weighting factor w for the commonly adopted network topologies and transmit constellations, respectively. We have tested the WC algorithm with ML detection using several different values of w for various scenarios and found that the proposed WC algorithm with the values of w between 0.25 and 2 usually performed well. Therefore, only the SEP of the WC algorithm with ML detection using $w = 0.25, 1, 2$ are provided in Tables III and IV, along with the selected w^* according to (24), highlighted in gray. In Table III, 16QAM is adopted and three asymmetric network topologies are considered, specifically: (a) $d_{sd} = \sqrt{2}d_{sr} = \sqrt{2}d_{rd}$, (b) $d_{sd} = 2d_{sr} = d_{rd}$, and (c) $d_{sd} = d_{sr} = 2d_{rd}$, which respectively stand for the case when the source is far from the destination, the case when the relay is near the source and the case when the relay is near the destination, as depicted in Fig. 2. In all these network topologies, the quality of the S-D link is worse than that of the S-R-D link. In Table IV, the transmit constellations utilized consist of QPSK, 8PSK and 16QAM, while a symmetric network topology is considered,

TABLE IV

SEP OF WC ALGORITHM WITH DIFFERENT VALUES OF w FOR COMMONLY ADOPTED TRANSMIT CONSTELLATIONS WITH $d_{\mathrm{SD}} = d_{\mathrm{SR}} = d_{\mathrm{RD}}$, $N = 2$

Transmit Constellation	w	$\mathrm{SNR_{sd}} = 8\mathrm{dB}$	$\mathrm{SNR_{sd}} = 16\mathrm{dB}$	$\mathrm{SNR_{sd}} = 24\mathrm{dB}$
QPSK	0.25	$9.07e^{-3}$	$3.06e^{-5}$	$3.7e^{-8}$
	1	$5.94e^{-3}$	$1.33e^{-5}$	$8.5e^{-9}$
	1.5	$5.62e^{-3}$	$1.22e^{-5}$	$8e^{-9}$
	2	$6.4e^{-3}$	$2.01e^{-5}$	$9e^{-9}$
8PSK	0.25	0.1098	$1.69e^{-3}$	$3.28e^{-6}$
	1	0.0901	$9.58e^{-4}$	$1.55e^{-6}$
	1.5	0.076	$9.46e^{-4}$	$9e^{-7}$
	2	0.092	$1.07e^{-3}$	$1.64e^{-6}$
16QAM	0.25	0.2703	$8.85e^{-3}$	$2.25e^{-5}$
	1	0.2378	$5.6e^{-3}$	$1.14e^{-5}$
	1.5	0.2356	$5.61e^{-3}$	$1.07e^{-5}$
	2	0.2362	$6.64e^{-3}$	$1.17e^{-5}$
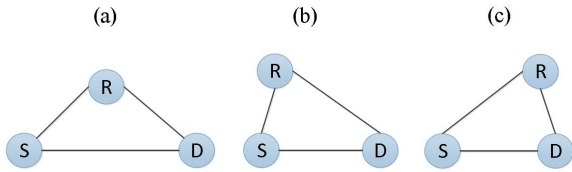
Fig. 2. Three asymmetric network topologies: (a) $d_{\mathrm{sd}} = \sqrt{2}d_{\mathrm{sr}} = \sqrt{2}d_{\mathrm{rd}}$, (b) $d_{\mathrm{sd}} = 2d_{\mathrm{sr}} = d_{\mathrm{rd}}$, and (c) $d_{\mathrm{sd}} = d_{\mathrm{sr}} = 2d_{\mathrm{rd}}$.
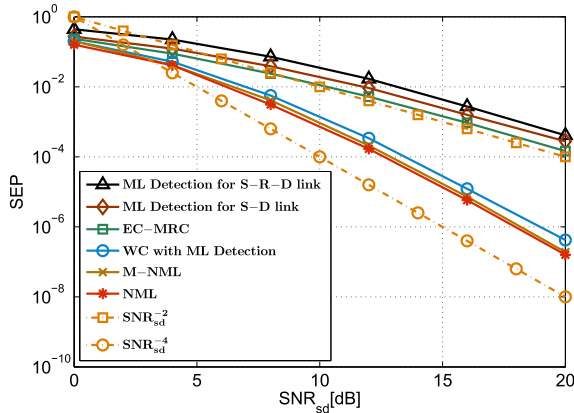

Fig. 3. SEP performance of different joint detection schemes and ML detections for S-D and S-R-D links with $N = 2$, QPSK and $d_{\mathrm{sd}} = d_{\mathrm{sr}} = d_{\mathrm{rd}}$.
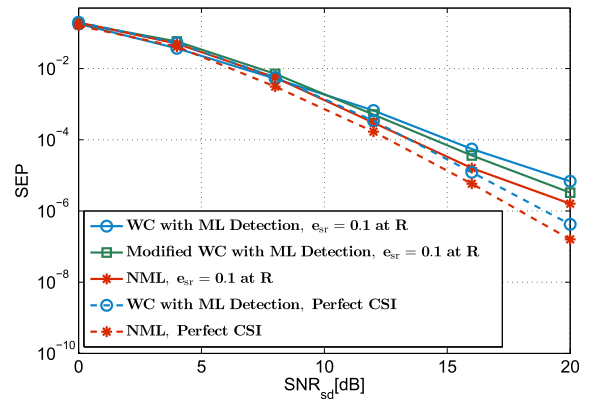

Fig. 4. The effect of erroneous estimation $\mathbf{H}_{\mathrm{sr}}$ at R on the SEP performance of joint detection schemes with QPSK, $N = 2$ and symmetric network topology.

i.e. $d_{\mathrm{sd}} = d_{\mathrm{sr}} = d_{\mathrm{rd}}$, for which the optimal value of w^* in (24) is equal to 1.5. It can be deduced from Tables III and IV that the selected value of the weighting factor in (24) leads to the best performance of the proposed WC algorithm for most cases, especially at high SNR. In particular, the use of w^* in (24) is significantly better than the value of 0.25 which is derived using the Chernoff bound approximation.

Fig. 3 compares the SEP performances of the proposed WC algorithm with ML detection and the benchmark joint detection schemes, including NML [20], M-NML [21] and EC-MRC [21] with $\alpha = 1$. Additionally, the SEP performances for the S-D and S-R-D links are provided in Fig. 3. In this experiment, the number of antennas is set to $N = 2$, and the transmit constellation is QPSK. For reference, two diversity curves corresponding to SNR^{-2} and SNR^{-4}, are also plotted in Fig. 3. As seen from this figure, the proposed

WC algorithm with ML detection, NML and M-NML schemes achieve the same diversity order equal to 4, which is twice than those of the EC-MRC scheme and the uncombined links. Moreover, the gap between the SEP performance of the WC algorithm with ML detection and that of the NML and M-NML schemes is tiny. This is because both the NML scheme and the proposed algorithm consider the effect of the error detection at R in the detection metric at D, and the performance loss caused by the relaxation of the search space for $\mathbf{e}$ (the step from (14) to (15)) in the proposed WC algorithm can be compensated by adaptively selecting w according to (24). Fig. 4 evaluates the effect of erroneous estimation of $\mathbf{H}_{\mathrm{sr}}$ at R on the SEP performance of the WC algorithm with ML detection and of the NML scheme. Specifically, it shows the SEP performance when the exact $\mathbf{H}_{\mathrm{sr}}$ is replaced by $\breve{\mathbf{H}}_{\mathrm{sr}} = \mathbf{H}_{\mathrm{sr}} + e_{\mathrm{sr}}\mathbf{E}$, where $\mathbf{E}$ denotes a random estimation error matrix which is uncorrelated to the channel matrix $\mathbf{H}_{\mathrm{sr}}$, and whose elements are i.i.d. ZMCSCG random variables with the same variance as that of $\mathbf{H}_{\mathrm{sr}}$, e_{sr} is a scaling factor set to 0.1, and QPSK is adopted with $N = 2$ and a symmetric network topology. As shown in Fig. 4, in the presence of imperfect CSI, the SEP of the WC algorithm with ML detection and of the NML scheme are worse than those with perfect CSI as the SNR increases. For the WC algorithm with ML detection, this performance loss can be reduced by changing the value
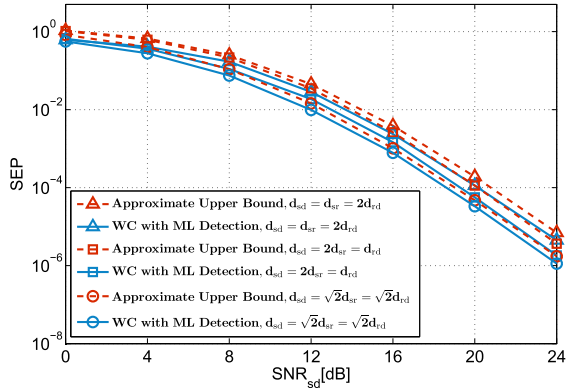
Fig. 5.   SEP performance of WC algorithm along with approximate upper bound (41) with $N = 2$ and 16QAM in asymmetric network topologies.
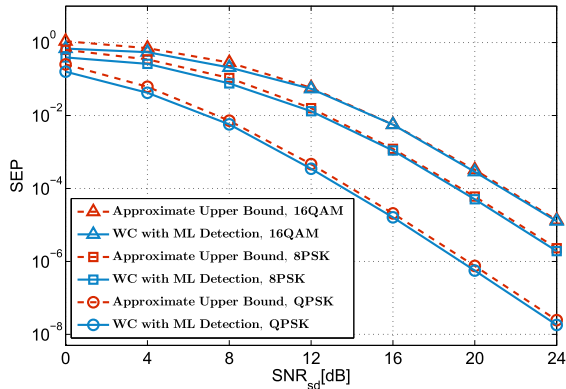

Fig. 6.   SEP performance of WC algorithm along with approximate upper bound (41) with $N = 2$, $d_{sd} = d_{sr} = d_{rd}$ and different transmit constellations.
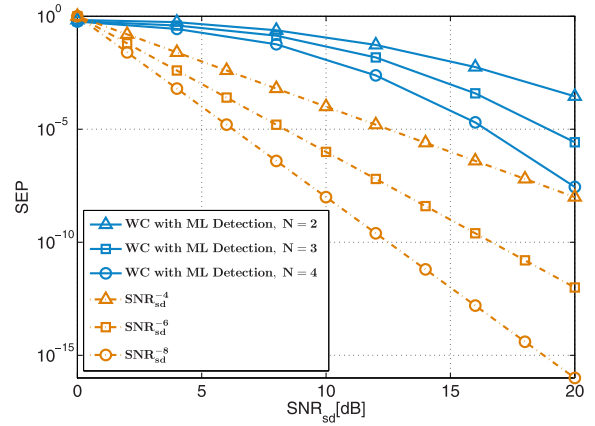

Fig. 7.   SEP performance of WC algorithm along with reference curves of diversity order with 16QAM, $d_{sd} = d_{sr} = d_{rd}$ and different antenna numbers.
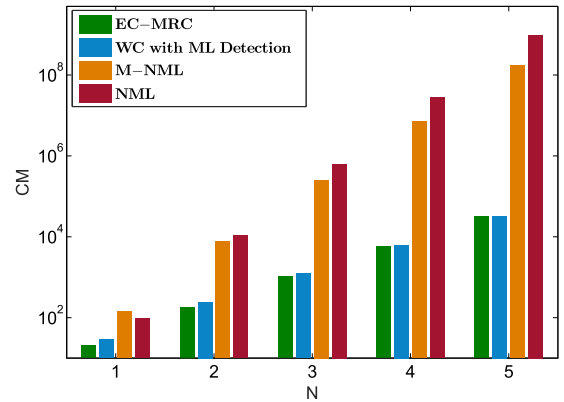

Fig. 8.   Comparison of computational complexity of different joint detection schemes versus antenna number N with $M = 2$.

of the weighting factor w. In the modified WC algorithm, we set $w = \frac{\sigma_{sr}^2/(\sigma_r^2 + e_{sr}\sigma_{sr}^2)}{\sigma_{sd}^2/\sigma_d^2}$ based on the knowledge of e_{sr} at D. While for the NML scheme, it is not possible to make such adjustment adaptively to the scenario with imperfect CSI. From this perspective, it can be deduced that the proposed WC algorithm with ML detection is more robust than the NML scheme. We can observe from Fig. 4 that the modification of w brings improvement to the WC algorithm at high SNR.

Figs. 5 and 6 test the accuracy of the derived approximate upper bound in (41) for different network topologies and transmit constellations when $N = 2$, respectively. Since the antenna configuration for these experiments satisfies both cases included in (41), we use their minimum value as the upper bound of SEP. In Fig. 5, the asymmetric network topologies as depicted in Fig. 2 and 16QAM are adopted. While in Fig. 6, the transmit constellations are QPSK, 8PSK and 16QAM and the symmetric network topology is adopted. We can observe from Fig. 5 that there is a small gap between the approximate upper bound and the SEP of the WC algorithm with ML detection in the high SNR regime. Furthermore, Fig. 5 shows that improving the quality of the S-R and R-D links evenly enables the WC algorithm to achieve better SEP performance than that by improving the quality of the S-R link or R-D link solely. For the experiment in Fig. 6, the derived approximate upper bound provides a close match to the SEP curves of the WC algorithm in the high SNR regime for various transmit constellations, especially the one with the high modulation order $M = \log_2 \Omega$. By comparing

Figs. 5 and 6, we can find that the derived upper bound of SEP is more accurate in the symmetric network topology than in asymmetric ones. As expected, it can also be observed from Fig. 6 that the SEP performance of the proposed WC algorithm is improved as M decreases, but the diversity order of the SM MIMO DF relaying systems with the WC algorithm is not affected by transmit constellations, which only depends on the antenna number as will be demonstrated in the following simulation. Fig. 7 displays the SEP curves of the WC algorithm with different numbers of antennas $N \in \{2, 3, 4\}$ and a 16QAM constellation. Moreover, three different diversity order curves corresponding to SNR^{-4}, SNR^{-6} and SNR^{-8} are included for reference. It can be observed from Fig. 7 that the SEP performance of the proposed WC algorithm becomes better as the number of antennas increases, and the validity of the derived diversity order formula in Section IV-B can be demonstrated by comparing the SEP performance of the WC algorithm with the reference SNR^{-p} ($p = 2, 4, 6$) curves in the high SNR regime.

B. Computational Complexity Evaluation

Figs. 8 and 9 display the computational complexity for the proposed WC algorithm and existing joint detection schemes, as evaluated based on the formulas given in Table II, versus the modulation order M and antenna number N, respectively. A QPSK constellation ($M = 2$) is adopted in Fig. 8 while the antenna number is set to $N = 2$ in Fig. 9. As shown

TABLE V
THE AVERAGE SIMULATION TIMES (IN SECONDS) OF DIFFERENT JOINT DETECTING SCHEMES

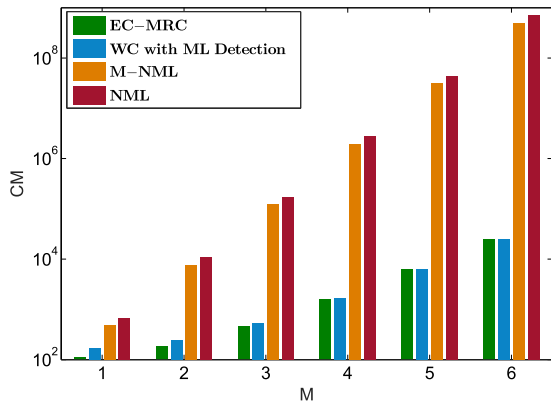|	Joint Detection Scheme	$N = 2$	$N = 3$	$N = 4$
QPSK ($M = 2$)	EC-MRC	0.0224	0.0386	0.1017
	WC with ML detection	0.0303	0.0459	0.1080
	M-NML	0.6249	4.9036	52.7922
	NML	0.8411	7.2548	79.1330
8PSK ($M = 3$)	EC-MRC	0.0421	0.1844	1.0143
	WC with ML detection	0.0503	0.1888	1.0552
	M-NML	4.9002	177.2306	8229.8414
	NML	7.2796	268.4578	12746.5396
16QAM ($M = 4$)	EC-MRC	0.0984	0.9699	11.8321
	WC with ML detection	0.1053	1.0302	12.1388
	M-NML	51.7268	8159.8890	$\gg$ 864000
	NML	81.0833	12663.1263	$\gg$ 864000

Fig. 9. Comparison of computational complexity of different joint detection schemes versus modulation order M with $N = 2$.

in Figs. 8 and 9, NML and its improvement M-NML exhibit a markedly higher complexity in comparison to WC. For instance, NML requires nearly 10^6 CM with $N = 3$ and $M = 2$ in Fig. 8, and 5×10^6 CM with $M = 4$ and $N = 2$ in Fig. 9, which is approximately a thousand time more than that for WC. In fact, the gap between NML or M-NML and WC becomes more remarkable as N and M increases. While the complexity of EC-MRC is comparable to that of the proposed WC algorithm, this is achieved at the expense of a significantly higher SEP, as previously shown in Fig. 3. Note that the main goal of our work was to present a new, simplified scheme for the joint signal detection in SM MIMO DF relay systems that can achieve comparable performance as the benchmark NML scheme but with much reduced computational complexity. As demonstrated by the SEP vs SNR results in Fig. 3 and the computational complexity results in Figs. 8 and 9, we believe that our goal has been achieved.

The averaged simulation times of the joint detection schemes considered in Figs. 8 and 9 are given in Table V for different values of N and M. For each experiment, 720 bits are transmitted and the run time of the detection process is measured using the Matlab functions "tic" and "toc". The computer hardware configuration used to run our simulation experiments consists of an 8 cores i7-6700 CUP operating at 3.4GHz along with 16GB of RAM. In each case, the simulation time is averaged over 10 experiments and presented

in seconds. It can be observed from Table V that the proposed WC algorithm with ML detection consumes slightly more time than EC-MRC, but significantly less time than NML and M-NML. As N and M increase, the averaged simulation time for the proposed WC algorithm with ML detection approaches that of EC-MRC and becomes nearly 0.01% of those for NML and M-NML; in effect, the latter schemes become impractical for SM MIMO DF relaying applications when $N = 4$ and 16QAM is used as the transmit constellation. Further comparison of the simulation times in Table V and the analytical complexity measures in Figs. 8 and 9 point to the validity of the complexity analysis presented in Section IV-C.

VI. CONCLUSIONS

In this paper, a new WC algorithm to be applied before the detector at the destination, was proposed and investigated for the SM MIMO DF relaying system. With the proposed WC algorithm, a combined signal vector and an equivalent channel matrix, which respectively have the same dimensions as those for the S-D link, were obtained. We analyzed the diversity order and computational complexity of the WC algorithm with ML detection. An approximate upper bound on the SEP for the WC algorithm with ML detection was also derived, based on the approximate upper bound for the PEP. Simulation results validated the theoretical analysis and consistency of the derived upper bound on the SEP. Furthermore, it was shown by simulations that in symmetric networks, the proposed WC algorithm with ML detection can provide a similar SEP performance as that of the benchmark NML detector, but with significantly lower complexity.

APPENDIX A
PROOF OF PROPOSITION 1

Since $\mathbf{e} = \check{\mathbf{x}} - \mathbf{x}$, (7) can be rewritten as

$$P(\mathbf{x} \to \check{\mathbf{x}}|\mathbf{H}_{sr}) = P(\mathbf{e}|\mathbf{H}_{sr}) = Q\left(\sqrt{\frac{\|\mathbf{H}_{sr}\mathbf{e}\|^2}{2\sigma_r^2}}\right). \quad (42)$$

The probability of the discrete random vector $\mathbf{e}$ can therefore be calculated by

$$P(\mathbf{e}) = \int P(\mathbf{e}|\mathbf{H}_{sr}) f(\mathbf{H}_{sr}) d\mathbf{H}_{sr}. \quad (43)$$
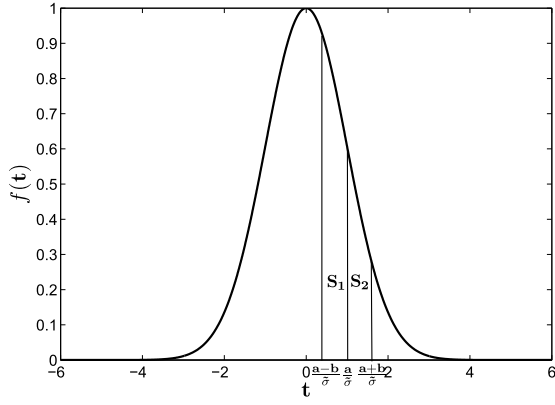
Fig. 10. Plot of the function $f(t) = \exp\left[-t^2/2\right]$.

From (42) and (43), we can find that $P(\mathbf{e}) = P(-\mathbf{e})$. Moreover, $P(\mathbf{x} \rightarrow \hat{\mathbf{x}}|\mathbf{H}_{\mathrm{sd}}, \mathbf{H}_{\mathrm{sr}}, \mathbf{H}_{\mathrm{rd}}, \mathbf{e} = \mathbf{0}) = Q\left(\frac{a}{\tilde{\sigma}}\right)$ can be obtained according to (30) and (32). Based on these observations, the conditional PEP based on $\mathbf{H}_{\mathrm{sd}}$, $\mathbf{H}_{\mathrm{sr}}$ and $\mathbf{H}_{\mathrm{rd}}$ can be computed as in (44) at the bottom of this page, where $\mathcal{F}^+ = \{\mathbf{e} \in \mathcal{E}^{N_{\mathrm{s}}}|\mathbf{e} \neq \mathbf{0}, b > 0\}$. Since $\frac{a}{\tilde{\sigma}} > 0$, it can be deduced that $S_1 - S_2 > 0$ with the help of Fig. 10. However, as the SNR of the S-R link increases, $P(\mathbf{e} \neq \mathbf{0}) \rightarrow 0$, i.e., $\mathbf{e} \rightarrow \mathbf{0}$, which can be obtained from (42) and (43). Moreover, as the SNR of

the S-D link increases, $\frac{a}{\tilde{\sigma}}$ becomes larger and $(S_1 - S_2) \rightarrow 0$. In summary,

$$P(\mathbf{x} \rightarrow \hat{\mathbf{x}}|\mathbf{H}_{\mathrm{sd}}, \mathbf{H}_{\mathrm{sr}}, \mathbf{H}_{\mathrm{rd}})$$
$$\gtrsim P(\mathbf{x} \rightarrow \hat{\mathbf{x}}|\mathbf{H}_{\mathrm{sd}}, \mathbf{H}_{\mathrm{sr}}, \mathbf{H}_{\mathrm{rd}}, \mathbf{e} = \mathbf{0}) = Q\left(\frac{a}{\tilde{\sigma}}\right), \quad (45)$$

and the approximation $Q\left(\frac{a}{\tilde{\sigma}}\right)$ can be reached in the high SNR regime for the S-R or S-D links. To simplify the computation of the conditional PEP, we only consider the asymptotic properties of the conditional PEP in (45), i.e., $P(\mathbf{x} \rightarrow \hat{\mathbf{x}}|\mathbf{H}_{\mathrm{sd}}, \mathbf{H}_{\mathrm{sr}}, \mathbf{H}_{\mathrm{rd}}) \approx Q\left(\frac{a}{\tilde{\sigma}}\right)$ in the high SNR regime of the S-R or S-D links. Under these conditions, the conditional PEP can be approximately upper bounded as in (46) on the bottom of this page, where (a) follows from the Chernoff bound [26] and (b) from the fact that $c > 0$.

APPENDIX B
PROOF OF PROPOSITION 2

We first re-express (35) as the following function

$$P(\mathbf{x} \rightarrow \hat{\mathbf{x}}|\mathbf{H}_{\mathrm{sd}}, \mathbf{H}_{\mathrm{sr}}, \mathbf{H}_{\mathrm{rd}})$$
$$< \frac{1}{2} \exp\left[-\frac{\|\mathbf{t}\|^2}{4\sigma_{\mathrm{d}}^2}\mathbf{v}^H\mathbf{H}_{\mathrm{sd}}^H\mathbf{H}_{\mathrm{sd}}\mathbf{v}\right]$$
$$\times \exp\left[-\frac{w\|\mathbf{t}\|^2}{4\sigma_{\mathrm{d}}^2}\mathbf{v}^H\mathbf{U}(\mathbf{I}_{N_{\mathrm{r}}}+\mathbf{T})\mathbf{T}\mathbf{U}^H\mathbf{H}_{\mathrm{sr}}^H\mathbf{H}_{\mathrm{sr}}\mathbf{v}\right], \quad (47)$$

$$P(\mathbf{x} \rightarrow \hat{\mathbf{x}}|\mathbf{H}_{\mathrm{sd}}, \mathbf{H}_{\mathrm{sr}}, \mathbf{H}_{\mathrm{rd}}) = Q\left(\frac{a}{\tilde{\sigma}}\right)P(\mathbf{e}=\mathbf{0}) + \sum_{\mathbf{e}\in\mathcal{E}^{N_{\mathrm{s}}}\setminus\{\mathbf{0}\}} Q\left(\frac{a+b}{\tilde{\sigma}}\right)P(\mathbf{e})$$

$$= Q\left(\frac{a}{\tilde{\sigma}}\right)P(\mathbf{e}=\mathbf{0}) + \sum_{\mathbf{e}\in\mathcal{E}^{N_{\mathrm{s}}}\setminus\{\mathbf{0}\}} \frac{1}{2\pi}\left[\int_{\frac{a}{\sigma}}^{\infty}\exp\left[-t^2/2\right]dt - \int_{\frac{a}{\sigma}}^{\frac{a+b}{\sigma}}\exp\left[-t^2/2\right]dt\right]P(\mathbf{e})$$

$$= Q\left(\frac{a}{\tilde{\sigma}}\right)P(\mathbf{e}=\mathbf{0}) + \sum_{\mathbf{e}\in\mathcal{E}^{N_{\mathrm{s}}}\setminus\{\mathbf{0}\}} Q\left(\frac{a}{\tilde{\sigma}}\right)P(\mathbf{e}) - \sum_{\mathbf{e}\in\mathcal{E}^{N_{\mathrm{s}}}\setminus\{\mathbf{0}\}} \frac{1}{2\pi}\int_{\frac{a}{\sigma}}^{\frac{a+b}{\sigma}}\exp\left[-t^2/2\right]dt\, P(\mathbf{e})$$

$$= Q\left(\frac{a}{\tilde{\sigma}}\right) + \sum_{\mathbf{e}\in\mathcal{F}^+}\left[\frac{1}{2\pi}\int_{\frac{a-b}{\sigma}}^{\frac{a}{\sigma}}\exp\left[-t^2/2\right]dt\, P(-\mathbf{e}) - \frac{1}{2\pi}\int_{\frac{a}{\sigma}}^{\frac{a+b}{\sigma}}\exp\left[-t^2/2\right]dt\, P(\mathbf{e})\right]$$

$$= Q\left(\frac{a}{\tilde{\sigma}}\right) + \sum_{\mathbf{e}\in\mathcal{F}^+}\frac{1}{2\pi}\left[\underbrace{\int_{\frac{a-b}{\sigma}}^{\frac{a}{\sigma}}\exp\left[-t^2/2\right]dt}_{S_1} - \underbrace{\int_{\frac{a}{\sigma}}^{\frac{a+b}{\sigma}}\exp\left[-t^2/2\right]dt}_{S_2}\right]P(\mathbf{e}) \quad (44)$$

$$P(\mathbf{x} \rightarrow \hat{\mathbf{x}}|\mathbf{H}_{\mathrm{sd}}, \mathbf{H}_{\mathrm{sr}}, \mathbf{H}_{\mathrm{rd}}) \overset{(a)}{\lesssim} \frac{1}{2}\exp\left[-\frac{a^2}{2\tilde{\sigma}^2}\right]$$

$$= \frac{1}{2}\exp\left[-\frac{1}{4\sigma_{\mathrm{d}}^2}\mathbf{t}^H\left(\mathbf{H}_{\mathrm{sd}}^H\mathbf{H}_{\mathrm{sd}} + \left(\mathbf{I}_{N_{\mathrm{r}}} + \mathbf{H}_{\mathrm{rd}}^H\mathbf{H}_{\mathrm{rd}}\Xi\right)\mathbf{H}_{\mathrm{rd}}^H\mathbf{H}_{\mathrm{rd}}\Xi w\mathbf{H}_{\mathrm{sr}}^H\mathbf{H}_{\mathrm{sr}}\right)\mathbf{t}\right.$$

$$\left.-\frac{\mathbf{t}^H\mathbf{H}_{\mathrm{rd}}^H\mathbf{H}_{\mathrm{rd}}\Xi\mathbf{H}_{\mathrm{rd}}^H\mathbf{H}_{\mathrm{rd}}\Xi w\mathbf{H}_{\mathrm{sr}}^H\mathbf{H}_{\mathrm{sr}}\mathbf{t}\mathbf{t}^H\mathbf{H}_{\mathrm{rd}}^H\mathbf{H}_{\mathrm{rd}}\Xi\mathbf{H}_{\mathrm{rd}}^H\mathbf{H}_{\mathrm{rd}}\Xi w\mathbf{H}_{\mathrm{sr}}^H\mathbf{H}_{\mathrm{sr}}\mathbf{t}}{\underbrace{4\sigma_{\mathrm{d}}^2\mathbf{t}^H\left(\mathbf{H}_{\mathrm{sd}}^H\mathbf{H}_{\mathrm{sd}} + w\mathbf{H}_{\mathrm{sr}}^H\mathbf{H}_{\mathrm{sr}}\Xi\mathbf{H}_{\mathrm{rd}}^H\mathbf{H}_{\mathrm{rd}}\Xi w\mathbf{H}_{\mathrm{sr}}^H\mathbf{H}_{\mathrm{sr}}\right)\mathbf{t}}_{c}}\right]$$

$$\overset{(b)}{<} \frac{1}{2}\exp\left[-\frac{1}{4\sigma_{\mathrm{d}}^2}\mathbf{t}^H\left(\mathbf{H}_{\mathrm{sd}}^H\mathbf{H}_{\mathrm{sd}} + \left(\mathbf{I}_{N_{\mathrm{r}}} + \mathbf{H}_{\mathrm{rd}}^H\mathbf{H}_{\mathrm{rd}}\Xi\right)\mathbf{H}_{\mathrm{rd}}^H\mathbf{H}_{\mathrm{rd}}\Xi w\mathbf{H}_{\mathrm{sr}}^H\mathbf{H}_{\mathrm{sr}}\right)\mathbf{t}\right] \quad (46)$$

$$P(\mathbf{x} \to \hat{\mathbf{x}}) < \underbrace{\frac{1}{2} \int \exp\left[-\frac{\|\mathbf{t}\|^2}{4\sigma_{\mathrm{d}}^2} \mathbf{v}^H \mathbf{H}_{\mathrm{sd}}^H \mathbf{H}_{\mathrm{sd}} \mathbf{v}\right] f(\mathbf{H}_{\mathrm{sd}}) \, d\mathbf{H}_{\mathrm{sd}}}_{P_{\mathrm{sd}}}$$

$$\times \underbrace{\iiint_{\mathbf{U}(n)} \exp\left[-\frac{w\|\mathbf{t}\|^2}{4\sigma_{\mathrm{d}}^2} \mathbf{v}^H \mathbf{U}(\mathbf{I}_{N_{\mathrm{r}_{\mathrm{t}}}} + \mathbf{T}) \mathbf{T} \mathbf{U}^H \mathbf{H}_{\mathrm{sr}}^H \mathbf{H}_{\mathrm{sr}} \mathbf{v}\right] f(\mathbf{T}) f(\mathbf{H}_{\mathrm{sr}}) \, D\mathbf{U} d\mathbf{T} d\mathbf{H}_{\mathrm{sr}}}_{P_{\mathrm{srd}}}, \qquad (48)$$

where $\mathbf{v} = \mathbf{t}/\|\mathbf{t}\|$ is a vector whose norm is one. Then the upper bound on the PEP in the high SNR regime for the S-R or S-D links can be calculated by averaging (47) w.r.t. $\mathbf{H}_{\mathrm{sd}}$, $\mathbf{H}_{\mathrm{sr}}$, $\mathbf{U}$ and $\mathbf{T}$ [26], which is given in (48) on the top of this page, where $\mathbf{U}(n)$ is the group of unitary matrices and $D\mathbf{U}$ denotes the standard Haar measure of $\mathbf{U}(n)$. It can be observed from (48) that the upper bound on the PEP in the high SNR regime for the S-R or S-D links contains two part, defined as P_{sd} and P_{srd}, which represent the upper bounds on the PEP of the S-D and S-R-D links, respectively. P_{sd} can be rewritten as

$$P_{\mathrm{sd}} = \int \exp\left[-\frac{\|\mathbf{t}\|^2}{4\sigma_{\mathrm{d}}^2}\|\mathbf{H}_{\mathrm{sd}}\mathbf{v}\|^2\right] f\left(\|\mathbf{H}_{\mathrm{sd}}\mathbf{v}\|^2\right) d\|\mathbf{H}_{\mathrm{sd}}\mathbf{v}\|^2. \quad (49)$$

Using the fact that $\|\mathbf{H}_{\mathrm{sd}}\mathbf{v}\|^2$ follows central Chi-square distribution, i.e.,

$$f\left(\|\mathbf{H}_{\mathrm{sd}}\mathbf{v}\|^2\right) = \frac{\|\mathbf{H}_{\mathrm{sd}}\mathbf{v}\|^{2N_{\mathrm{d}}-2}}{\sigma_{\mathrm{sd}}^{2N_{\mathrm{d}}} \Gamma(N_{\mathrm{d}})} \exp\left[-\|\mathbf{H}_{\mathrm{sd}}\mathbf{v}\|^2/\sigma_{\mathrm{sd}}^2\right], \quad (50)$$

(49) can be calculated by

$$P_{\mathrm{sd}} = \left(1 + \frac{\|\mathbf{t}\|^2 \sigma_{\mathrm{sd}}^2}{4\sigma_{\mathrm{d}}^2}\right)^{-N_{\mathrm{d}}}. \quad (51)$$

For the calculation of P_{srd}, we first rewrite it as follows:

$$P_{\mathrm{srd}} = \iiint_{\mathbf{U}(n)} \exp[\mathrm{Tr}(-\frac{w\|\mathbf{t}\|^2}{4\sigma_{\mathrm{d}}^2} \mathbf{U}^H \mathbf{H}_{\mathrm{sr}}^H \mathbf{H}_{\mathrm{sr}} \mathbf{v} \mathbf{v}^H \mathbf{U}$$
$$\times (\mathbf{I}_{N_{\mathrm{r}_{\mathrm{t}}}} + \mathbf{T})\mathbf{T})] f(\mathbf{T}) f(\mathbf{H}_{\mathrm{sr}}) \, D\mathbf{U} d\mathbf{T} d\mathbf{H}_{\mathrm{sr}}. \quad (52)$$

Since $\mathbf{H}_{\mathrm{sr}}^H \mathbf{H}_{\mathrm{sr}} \mathbf{v} \mathbf{v}^H$ has only one eigenvalue $\varsigma = \|\mathbf{H}_{\mathrm{sr}}\mathbf{v}\|^2$ and $(\mathbf{I}_{N_{\mathrm{r}_{\mathrm{t}}}} + \mathbf{T})\mathbf{T}$ has the eigenvalue $(1 + \lambda_i)\lambda_i$, (52) can be calculated based on the unitary integral result of Equ. (16) in [31] as

$$P_{\mathrm{srd}} = \int \cdots \iint \frac{m^{-(N_{\mathrm{s}}-1)}(N_{\mathrm{s}}-1)!}{\varsigma^{N_{\mathrm{s}}-1} \Delta\left((\lambda+1)\lambda\right)}$$
$$\times \det_{N_{\mathrm{s}}} \begin{bmatrix} \exp[m(1+\lambda_k)\lambda_k \varsigma]\,|_{j=1} \\ [(1+\lambda_k)\lambda_k]^{N_{\mathrm{s}}-j}\,|_{j=2,\ldots,N_{\mathrm{s}}} \end{bmatrix}$$
$$\times f(\varsigma) f(\lambda_1) \ldots f(\lambda_{N_{\mathrm{s}}}) \, d\varsigma d\lambda_1 \ldots d\lambda_{N_{\mathrm{s}}}$$
$$= \int \cdots \iint m^{-(N_{\mathrm{s}}-1)}(N_{\mathrm{s}}-1)!$$
$$\times \sum_{i=1}^{N_{\mathrm{s}}} \frac{\exp[m(1+\lambda_i)\lambda_i \varsigma]}{\varsigma^{N_{\mathrm{s}}-1} \prod_{1 \leqslant j \leqslant N_{\mathrm{s}}, \, j \neq i} (1+\lambda_i)\lambda_i - (1+\lambda_j)\lambda_j}$$
$$\times f(\varsigma) d\varsigma f(\lambda_1) \ldots f(\lambda_{N_{\mathrm{s}}}) d\lambda_1 \ldots d\lambda_{N_{\mathrm{s}}}, \quad (53)$$

where $m = -w\|\mathbf{t}\|^2/(4\sigma_{\mathrm{d}}^2)$. Since ς follows the central Chi-square distribution

$$f(\varsigma) = \frac{\varsigma^{N_{\mathrm{r}_{\mathrm{r}}}-1}}{\sigma_{\mathrm{sr}}^{2N_{\mathrm{r}_{\mathrm{r}}}} \Gamma(N_{\mathrm{r}_{\mathrm{r}}})} \exp\left[-\varsigma/\sigma_{\mathrm{sr}}^2\right], \quad (54)$$

and using the fact that $\int_0^\infty t^n \exp[-\mu t] dt = n! \mu^{-n-1}$, (53) can be further derived as

$$P_{\mathrm{srd}} = \int \cdots \int \frac{m^{-(N_{\mathrm{s}}-1)}(N_{\mathrm{s}}-1)!}{\sigma_{\mathrm{sr}}^{2N_{\mathrm{r}_{\mathrm{r}}}} \Gamma(N_{\mathrm{r}_{\mathrm{r}}})}$$
$$\times \sum_{i=1}^{N_{\mathrm{s}}} \frac{(N_{\mathrm{r}_{\mathrm{r}}} - N_{\mathrm{s}})!}{\prod_{1 \leq j \leq N_{\mathrm{s}}, \, j \neq i} (1+\lambda_i)\lambda_i - (1+\lambda_j)\lambda_j}$$
$$\times \left(-m(1+\lambda_i)\lambda_i + \frac{1}{\sigma_{\mathrm{sr}}^2}\right)^{-N_{\mathrm{r}_{\mathrm{r}}}+N_{\mathrm{s}}-1}$$
$$\times f(\lambda_1) \ldots f(\lambda_{N_{\mathrm{s}}}) d\lambda_1 \ldots d\lambda_{N_{\mathrm{s}}}. \quad (55)$$

When $N_{\mathrm{r}_{\mathrm{r}}} = N_{\mathrm{s}}$, (55) is simplified as

$$P_{\mathrm{srd}} = \int \cdots \int (m\sigma_{\mathrm{sr}}^2)^{-(N_{\mathrm{s}}-1)}$$
$$\times \sum_{i=1}^{N_{\mathrm{s}}} \frac{\left(-m\sigma_{\mathrm{sr}}^2(1+\lambda_i)\lambda_i + 1\right)^{-1}}{\prod_{1 \leq j \leq N_{\mathrm{s}}, \, j \neq i} (1+\lambda_i)\lambda_i - (1+\lambda_j)\lambda_j}$$
$$\times f(\lambda_1) \ldots f(\lambda_{N_{\mathrm{s}}}) d\lambda_1 \ldots d\lambda_{N_{\mathrm{s}}}$$
$$\stackrel{(c)}{=} \prod_{i=1}^{N_{\mathrm{s}}} \int \left(-m\sigma_{\mathrm{sr}}^2(1+\lambda_i)\lambda_i + 1\right)^{-1} f(\lambda_i) d\lambda_i, \quad (56)$$

where (c) follows from the fact that

$$\sum_{i=1}^{N} (ax_i + 1)^{-1} \prod_{1 \leq j \leq N, \, j \neq i} (x_i - x_j)^{-1}$$
$$= (-a)^{N-1} \prod_{i=1}^{N} (ax_i + 1)^{-1}, \quad (57)$$

which is proved in Appendix C and here $x_i = (1+\lambda_i)\lambda_i$ is set. Moreover, replacing $\mathbf{H}_{\mathrm{rd}}^H \mathbf{H}_{\mathrm{rd}} \Xi \mathbf{H}_{\mathrm{sr}}^H \mathbf{H}_{\mathrm{sr}}$ and $\mathbf{H}_{\mathrm{rd}}^H \mathbf{H}_{\mathrm{rd}} \Xi$ in (33) with $\mathbf{H}_{\mathrm{sr}}^H \mathbf{H}_{\mathrm{sr}} \Xi \mathbf{H}_{\mathrm{rd}}^H \mathbf{H}_{\mathrm{rd}}$ and $\mathbf{I}_{N_{\mathrm{s}}} - w\mathbf{H}_{\mathrm{sr}}^H \mathbf{H}_{\mathrm{sr}} \Xi$ respectively and adopting the Schur decomposition of the complex square matrix $w\mathbf{H}_{\mathrm{sr}}^H \mathbf{H}_{\mathrm{sr}} \Xi = \mathbf{Q} \mathbf{R} \mathbf{Q}^H$, P_{srd} can be alternatively

expressed as

$$
\begin{aligned}
P_{\text{srd}} &= \iiint_{\mathbf{Q}(n)} \exp\left[-\frac{\|\mathbf{t}\|^2}{4\sigma_d^2}\mathbf{v}^H\mathbf{Q}(2\mathbf{I}_{N_s}-\mathbf{R})\mathbf{R}\mathbf{Q}^H\mathbf{H}_{\text{rd}}^H\mathbf{H}_{\text{rd}}\mathbf{v}\right] \\
&\quad \times f(\mathbf{R})f(\mathbf{H}_{\text{rd}})\,D\mathbf{Q}d\mathbf{R}d\mathbf{H}_{\text{rd}} \\
&= \iiint_{\mathbf{Q}(n)} \exp\left[\text{Tr}(-\frac{\|\mathbf{t}\|^2}{4\sigma_d^2}\mathbf{Q}^H\mathbf{H}_{\text{rd}}^H\mathbf{H}_{\text{rd}}\mathbf{v}\mathbf{v}^H\mathbf{Q}(2\mathbf{I}_{N_s}-\mathbf{R})\mathbf{R})\right] \\
&\quad \times f(\mathbf{R})f(\mathbf{H}_{\text{rd}})\,D\mathbf{Q}d\mathbf{R}d\mathbf{H}_{\text{rd}},
\end{aligned} \tag{58}
$$

where $\mathbf{R}$ and $\mathbf{Q}$ denote an upper-triangular matrix whose diagonal elements are η_i, $i = 1\ldots, N_s$ when $N_d, N_{r_r} \geqslant N_s$ and a unitary matrix, respectively. Using a similar approach as in the derivation of (52) above, (58) can be calculated as follows on the condition that $N_{r_r} \geqslant N_d = N_s$.

$$
P_{\text{srd}} = \prod_{i=1}^{N_s} \int \left(\|\mathbf{t}\|^2\sigma_{\text{rd}}^2(2-\eta_i)\eta_i/4\sigma_d^2 + 1\right)^{-1} f(\eta_i)d\eta_i. \tag{59}
$$

In summary, (36) is thereby proved.

APPENDIX C
PROOF OF EQUATION (57)

We first write (57) into the form $\sum_{i=1}^{N}(ax_i+1)^{-1}\prod_{1 \leq j \leq N_s,\, j \neq i}(x_i - x_j)^{-1} = \det \mathbf{A}_N/\det \mathbf{B}_N$, where the elements of matrices $\mathbf{A}_N$ and $\mathbf{B}_N$ are $[\mathbf{A}_N]_{j,k} = \begin{cases}(ax_k+1)^{-1}, & j=1 \\ x_k^{N-j}, & otherwise\end{cases}$ and $[\mathbf{B}_N]_{j,k} = x_k^{N-j}$, and then use mathematical induction to prove the desired result.

A. Basis

When $N = 2$,

$$
\begin{aligned}
\det \mathbf{A}_2/\det \mathbf{B}_2 &= [(ax_1+1)^{-1} - (ax_2+1)^{-1}]/(x_1 - x_2) \\
&= -a(ax_1+1)^{-1}(ax_2+1)^{-1}
\end{aligned}
$$

satisfies (57).

B. Inductive Step

When $N \geqslant 2$, assume $\det \mathbf{A}_{N-1}/\det \mathbf{B}_{N-1} = (-a)^{N-2}\prod_{i=1}^{N-1}(ax_i+1)^{-1}$ and transform $\det \mathbf{A}_N/\det \mathbf{B}_N = -\det \mathbf{A}/\det \mathbf{B}$, where

$$
\mathbf{A} = \begin{bmatrix} \mathbf{A}_{N-1} & \mathbf{b}_1 \\ \mathbf{c}_1 & x_N^{N-2} \end{bmatrix}, \quad \mathbf{B} = \begin{bmatrix} \mathbf{B}_{N-1} & \mathbf{b}_2 \\ \mathbf{c}_2 & x_N^{N-1} \end{bmatrix},
$$

$\mathbf{b}_1 = [(ax_N+1)^{-1}, x_N^{N-3}, \ldots, 1]^T$, $\mathbf{b}_2 = [x_N^{N-2}, x_N^{N-3}, \ldots, 1]^T$, $\mathbf{c}_1 = [x_1^{N-2}, x_2^{N-2}, \ldots, x_{N-1}^{N-2}]$ and $\mathbf{c}_2 = [x_1^{N-1}, x_2^{N-1}, \ldots, x_{N-1}^{N-1}]$. Therefore

$$
\begin{aligned}
\frac{\det \mathbf{A}_N}{\det \mathbf{B}_N} &= \frac{-\det(\mathbf{A}_{N-1} - x_N^{2-N}\mathbf{b}_1\mathbf{c}_1)x_N^{N-2}}{\det(\mathbf{B}_{N-1} - x_N^{1-N}\mathbf{b}_1\mathbf{c}_1)x_N^{N-1}} \\
&= \frac{-a\det(\mathbf{A}_{N-1})}{(ax_N+1)\det(\mathbf{B}_{N-1})} \\
&= (-a)^{N-1}\prod_{i=1}^{N}(ax_i+1)^{-1},
\end{aligned} \tag{60}
$$

and (57) is proved.

## REFERENCES

[1] K. Zhang, J. Wang, J. Yang, B. Champagne, and J. Wei, "A weighted combining algorithm for spatial multiplexing MIMO DF relaying systems," in *Proc. IEEE Veh. Technol. Conf. (VTC) Fall*, Montreal, QC, Canada, Sep. 2016, pp. 1–6.

[2] P. Bhat *et al.*, "LTE-advanced: An operator perspective," *IEEE Commun. Mag.*, vol. 50, no. 2, pp. 104–114, Feb. 2012.

[3] M. Baker, "From LTE-advanced to the future," *IEEE Commun. Mag.*, vol. 50, no. 2, pp. 116–120, Feb. 2012.

[4] S. Ma, Y. Yang, and H. Sharif, "Distributed MIMO technologies in cooperative wireless networks," *IEEE Commun. Mag.*, vol. 49, no. 5, pp. 78–82, May 2011.

[5] R. Zhang *et al.*, "Advances in base- and mobile-station aided cooperative wireless communications: An overview," *IEEE Veh. Technol. Mag.*, vol. 8, no. 1, pp. 57–69, Mar. 2013.

[6] J. Yang, B. Champagne, Y. Zou, and L. Hanzo, "Joint optimization of transceiver matrices for MIMO-aided multiuser AF relay networks: Improving the QoS in the presence of CSI errors," *IEEE Trans. Veh. Technol.*, vol. 65, no. 3, pp. 1434–1451, Mar. 2016.

[7] K. Jayasinghe, P. Jayasinghe, N. Rajatheva, and M. Latva-Aho, "Linear precoder-decoder design of MIMO device-to-device communication underlaying cellular communication," *IEEE Trans. Commun.*, vol. 62, no. 12, pp. 4304–4319, Dec. 2014.

[8] G. V. V. Sharma, V. Ganwani, U. B. Desai, and S. N. Merchant, "Performance analysis of maximum likelihood detection for decode and forward MIMO relay channels in Rayleigh fading," *IEEE Trans. Wireless Commun.*, vol. 9, no. 9, pp. 2880–2889, Sep. 2010.

[9] A. Bansal, M. R. Bhatnagar, A. Hjørungnes, and Z. Han, "Low-complexity decoding in DF MIMO relaying system," *IEEE Trans. Veh. Technol.*, vol. 62, no. 3, pp. 1123–1137, Mar. 2013.

[10] P. Clarke and R. C. de Lamare, "Transmit diversity and relay selection algorithms for multirelay cooperative MIMO systems," *IEEE Trans. Veh. Technol.*, vol. 61, no. 3, pp. 1084–1098, Mar. 2012.

[11] M. R. Bhatnagar and M. K. Arti, "Selection beamforming and combining in decode-and-forward MIMO relay networks," *IEEE Commun. Lett.*, vol. 17, no. 8, pp. 1556–1559, Aug. 2013.

[12] H.-B. Kong, C. Song, H. Park, and I. Lee, "A new beamforming design for MIMO AF relaying systems with direct link," *IEEE Trans. Commun.*, vol. 62, no. 7, pp. 2286–2295, Jul. 2014.

[13] V. S. Krishna and M. R. Bhatnagar, "A joint antenna and path selection technique in single-relay-based DF cooperative MIMO networks," *IEEE Trans. Veh. Technol.*, vol. 65, no. 3, pp. 1340–1353, Mar. 2016.

[14] T. Wang, A. Cano, G. B. Giannakis, and J. N. Laneman, "High-performance cooperative demodulation with decode-and-forward relays," *IEEE Trans. Commun.*, vol. 55, no. 7, pp. 1427–1438, Jul. 2007.

[15] A. Nasri, R. Schober, and M. Uysal, "Enhanced MRC for decode-and-forward cooperative diversity systems," *IEEE Trans. Wireless Commun.*, vol. 11, no. 10, pp. 3418–3423, Oct. 2012.

[16] A. Bansal, M. R. Bhatnagar, and A. Hjørungnes, "Decoding and performance bound of demodulate-and-forward based distributed Alamouti STBC," *IEEE Trans. Wireless Commun.*, vol. 12, no. 2, pp. 702–713, Feb. 2013.

[17] Y. Song, H. Shin, and E.-K. Hong, "MIMO cooperative diversity with scalar-gain amplify-and-forward relaying," *IEEE Trans. Commun.*, vol. 57, no. 7, pp. 1932–1938, Jul. 2009.

[18] C. Song, K.-J. Lee, and I. Lee, "Diversity-multiplexing tradeoff analysis for MMSE-based cooperative MIMO relaying systems," in *Proc. IEEE Int. Conf. Commun. (ICC)*, Ottawa, ON, Canada, Jun. 2012, pp. 4808–4812.

[19] K. Zhang, C. Xiong, B. Chen, J. Wang, and J. Wei, "A maximum likelihood combining algorithm for spatial multiplexing MIMO amplify-and-forward relaying systems," *IEEE Trans. Veh. Technol.*, vol. 64, no. 12, pp. 5767–5774, Dec. 2015.

[20] X. Jin, J.-S. No, and D.-J. Shin, "Relay selection for decode-and-forward cooperative network with multiple antennas," *IEEE Trans. Wireless Commun.*, vol. 10, no. 12, pp. 4068–4079, Dec. 2011.

[21] H. M. Kim, T. K. Kim, M. Min, and G. H. Im, "Low-complexity detection scheme for cooperative MIMO systems with decode-and-forward relays," *IEEE Trans. Commun.*, vol. 63, no. 1, pp. 94–106, Jan. 2015.

[22] T. Kong and Y. Hua, "Optimal design of source and relay pilots for MIMO relay channel estimation," *IEEE Trans. Signal Process.*, vol. 59, no. 9, pp. 4438–4446, Sep. 2012.

[23] Y. Rong, M. R. A. Khandaker, and Y. Xiang, "Channel estimation of dual-hop MIMO relay system via parallel factor analysis," *IEEE Trans. Wireless Commun.*, vol. 11, no. 6, pp. 2224–2233, Jun. 2012.

[24] K. Kreutz-Delgado. (Jun. 2009). "The complex gradient operator and the CR-calculus." [Online]. Available: https://arxiv.org/abs/0906.4835

[25] A. M. Chan and I. Lee, "A new reduced-complexity sphere decoder for multiple antenna systems," in *Proc. IEEE Int. Conf. Commun. (ICC)*, New York, NY, USA, Apr./May 2002, pp. 460–464.

[26] M. K. Simon and M.-S. Alouini, *Digital Communication Over Fading Channels*, 2nd ed. New York, NY, USA: Wiley, 2005.

[27] K. Kusume, M. Joham, and W. Utschick, "MMSE block decision-feedback equalizer for spatial multiplexing with reduced complexity," in *Proc. IEEE Global Commun. Conf. (GLOBECOM)*, Dallas, TX, USA, Nov./Dec. 2004, pp. 2540–2544.

[28] A. A. Khan, M. Naeem, and S. I. Shah, "A particle swarm algorithm for symbols detection in wideband spatial multiplexing systems," in *Proc. Genetic Evol. Comput. Conf. (GECC)*, New York, NY, USA, Jul. 2007, pp. 63–69.

[29] X. Guan, W. Yang, and Y. Cai, "Outage performance of statistical CSI assisted cognitive relay with interference from primary user," *IEEE Commun. Lett.*, vol. 17, no. 7, pp. 1416–1419, Jul. 2013.

[30] S. Kumar. (Jul. 2015). "Gap probabilities and densities of extreme eigenvalues of random matrices: Exact results." [Online]. Available: https://arxiv.org/abs/1507.08830

[31] A. Ghaderipoor, C. Tellambura, and A. Paulraj, "On the application of character expansions for MIMO capacity analysis," *IEEE Trans. Inf. Theory*, vol. 58, no. 5, pp. 2950–2962, May 2012.

Kangli Zhang (S'16) received the B.S. degree in communication engineering and the M.S. degree in information and communication engineering from the National University of Defense Technology, Changsha, China, in 2011 and 2013, respectively, where she is currently pursuing the Ph.D. degree with the College of Electronic Science and Engineering. From 2015 to 2016, she studied at the Statistical Signal Processing Laboratory, McGill University, Montreal, Canada, as a Visiting Ph.D. Student. Her research interests include signal processing for wireless communications with emphasis on the multiple-input multiple-output systems and cooperative communications.
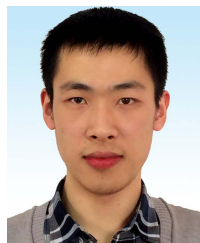
Jian Wang (S'16) received the B.S. degree in communication engineering from the National University of Defense Technology, Changsha, China, in 2012, where he is currently pursuing the Ph.D. degree with the College of Electronic Science and Engineering. From 2015 to 2016, he studied at the Integrated Systems Laboratory, Swiss Federal Institute of Technology (ETH), Zurich, as a Visiting Ph.D. Student. His research interests are in the area of signal processing and VLSI design for communication systems.
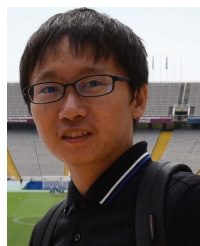
Jiaxin Yang (S'11) received the B.Eng. degree in information engineering from Shanghai Jiao Tong University, Shanghai, China, in 2009, and the M.E.Sc. degree in electrical and computer engineering from the University of Western Ontario, London, Canada, in 2011. He is currently pursuing the Ph.D. degree with the Department of Electrical and Computer Engineering, McGill University, Montreal, Canada. From 2015 to 2017, he was a Wireless System Research Intern with InterDigital. His research interests include optimization theory, statistical signal processing, detection and estimation, and the applications thereof in wireless communications, such as MIMO systems, cooperative communications, and physical-layer security.

Mr. Yang was a recipient of several awards and scholarships, including the Best Paper Award of 27th IEEE International Symposium on Personal, Indoor and Mobile Radio Communications, the McGill Engineering Doctoral Award, the Graduate Excellence Fellowship, the International Differential Tuition Fee Waivers, the FRQNT International Internship Scholarship, the PERSWADE Ph.D. Scholarship, the Graduate Research Enhancement and Travel Awards, and the Graduate Research Mobility Awards.

Benoit Champagne (S'87–M'89–SM'03) received the B.Ing. degree in engineering physics from the Cole Polytechnique de Montral in 1983, the M.Sc. degree in physics from the Universit de Montral in 1985, and the Ph.D. degree in electrical engineering from the University of Toronto in 1990. From 1990 to 1999, he was an Assistant and then Associate Professor with INRS-Telecommunications, Universit du Quebec, Montral. In 1999, he joined McGill University, Montreal, where he is currently a Full Professor with the Department of Electrical and Computer Engineering and also served as an Associate Chairman of Graduate Studies with the department from 2004 to 2007. His research has been funded by the Natural Sciences and Engineering Research Council of Canada, the Fonds de Recherche sur la Nature et les Technologies from the Government of Quebec, and some major industrial sponsors, including Nortel Networks, Bell Canada, InterDigital, and Microsemi. His research focuses on the study of advanced algorithms for the processing of communication signals by digital means. His interests span many areas of statistical signal processing, including detection and estimation, sensor array processing, adaptive filtering, and applications thereof to broadband communications and audio processing, where he has co-authored over 250 referred publications.

Dr. Champagne has served on the technical committees of several international conferences in the fields of communications and signal processing. He was the Registration Chair of the IEEE ICASSP 2004, the Co-Chair of the Antenna and Propagation Track for the IEEE VTCFall 2004, the Co-Chair of the Wide Area Cellular Communications Track for the IEEE PIMRC 2011, the Co-Chair of the Workshop on D2D Communications for the IEEE ICC 2015, and the Publicity Chair of the IEEE VTCFall 2016. He was an Associate Editor of the *EURASIP Journal on Applied Signal Processing* from 2005 to 2007, the IEEE SIGNAL PROCESSING LETTERS from 2006 to 2008, and the IEEE TRANSACTIONS ON SIGNAL PROCESSING from 2010 to 2012, and a Guest Editor for two special issues of the *EURASIP Journal on Applied Signal Processing* published in 2007 and 2014.
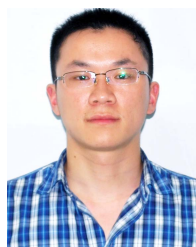
Fanglin Gu received the B.S. degree in communication engineering and the Ph.D. degree in information and communication engineering from the PLA University of Science and Technology, Nanjing, China, in 2008 and 2013, respectively. He is currently a Lecturer with the Communication Engineering Department, National University of Defense Technology, Changsha, China. His research interests are in the area of signal processing for communications.

Jibo Wei (M'04) received the B.S. and M.S. degrees from the National University of Defense Technology (NUDT), Changsha, China, in 1989 and 1992, respectively, and the Ph.D. degree from Southeast University, Nanjing, China, in 1998, all in electronic engineering. He is currently a Professor with the Department of Communication Engineering, NUDT. His research interests include design and optimization of communication systems and signal processing in communications, more specially, the areas of MIMO, multicarrier transmission, cooperative communication, and cognitive network.

Dr. Wei is a member of the IEEE Communication Society and also a member of the IEEE Vehicular Technology Society. He is a Senior Member of the China Institute of Communications and Electronics. He is also an Editor of the *Journal on Communications*.